Supporting information

Insertion Polymerization of Acrylate

Damien Guironnet, Philipp Roesle, Thomas Rünzi, Inigo Göttker-Schnetmann, and Stefan Mecking*

University of Konstanz, Chair of Chemical Materials Science, Dept. of Chemistry, 78457 Konstanz, Germany

Contents:

I. Materials and General Considerations

Unless noted otherwise, all manipulations of nickel and palladium complexes were carried out under an inert atmosphere using standard glovebox or Schlenk techniques. All glassware was flame-dried under vacuum before use. Toluene was distilled from sodium, diethylether, dioxane, and THF from sodium / benzophenone ketyl under argon. DMSO and methylene chloride were distilled from CaH_2. [(tmeda)$NiMe_2$] was supplied by MCAT (Konstanz, Germany). Ethylene (3.5 grade) supplied by Praxair and methyl acrylate supplied by Aldrich were used as received. [(tmeda)$PdMe_2$][1], [2-(2-methoxyphenyl)phosphino]benzenesulphonic acid[2], [2-(2-(2',6'-dimethoxyphenyl) phenyl) phosphino] benzenesulphonic acid[3] and the corresponding **2b-TMEDA**[3], **1a-TMEDA**[4]**, 2a-lut**[5] and **1a-pyr**[4] were synthesized by known procedures.

NMR spectra were recorded on a Varian Unity INOVA 400 or on a Bruker Avance DRX 600 spectrometer. ^1H and ^{13}C NMR chemical shifts were referenced to the solvent signal. Multiplicities are given as follows (or combinations thereof): s: singlet, d: doublet, t: triplet, vt: virtual triplet, m: multiplet. The identity and purity of metal complexes was established by ^1H, ^{13}C and ^{31}P NMR, and elemental analysis. NMR assignments were confirmed by ^1H, ^1H gCOSY, ^1H, ^{13}C gHSQC and ^1H, ^{13}C gHMBC experiments. High-temperature NMR measurements of polyethylenes were performed in 1,1,2,2-tetrachloroethane-d_2 at 130 °C. For ethylene homopolymers and ethylene-methyl acrylate copolymers with a moderate acrylate incorporation, gel permeation chromatography (GPC) was carried out in 1,2,4-trichlorobenzene at 160°C at a flow rate of 1 mL min^{-1} on a Polymer Laboratories 220 instrument equipped with Olexis columns with differential refractive index-, viscosity- and light scattering- (15° and 90°) detectors. Data reported were determined via triple detection employing the PL GPC220 software algorithm. As the instrument records light scattering at only two angles, data analysis involves an iteration for the calculation of molecular weights and form factors for each measured interval. The instrument was calibrated with narrow polystyrene and polyethylene standards. Data given is referenced to linear polyethylene. For copolymers with a high acrylate incorporation, molecular weights were determined by GPC on a polymer laboratories PL-GPC 50 instrument with two PLgel 5 µm MIXED-C columns and an RI-detector in THF against polystyrene standard.

II. Complex syntheses

A. Bis{*N,N'*-{(κ^2-*P,O*)-2-[di(2-methoxyphenyl)phosphino]benzenesulphonato} palladium(II)-methyl}-*N,N,N',N'*-tetramethylethylenediamine (2a-TMEDA)

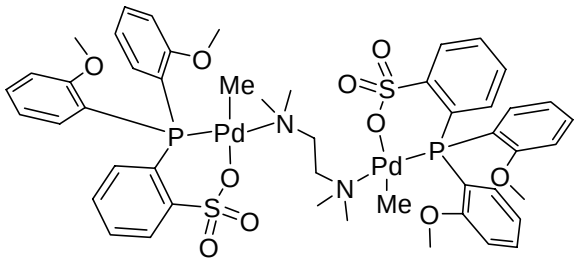

1.00 g (2.49 mmol) of [2-(2-methoxyphenyl)phosphino]benzenesulphonic acid and 0.63 g (2.49 mmol) of [(tmeda)$PdMe_2$] were dissolved in dioxane. Gas evolution was observed, followed by immediate precipitation of the product. The solution was stirred for 60 minutes at room temperature. The white precipitate was filtered off, washed with diethyl ether and dried under reduced pressure to yield 1.40 g (1.22 mmol, 98%) of **2a-TMEDA**. The low solubility of the complex hampered analysis by ^{13}C NMR. ^1H NMR (400 MHz, DMSO-d_6) δ = 7.7-6.8 (m, 20H), 6.35 (m, 4H), 3.49 (s, 12H, OCH_3), 2.30 (s, 4H, NCH_2), 2.13 (s, 12H, NCH_3), 0.10 (6H, Pd-CH_3).

B. {(κ^2-*P,O*)-2-[Di(2-methoxyphenyl)phosphino]benzenesulphonato} pyridine palladium(II)-methyl (2a-pyr)

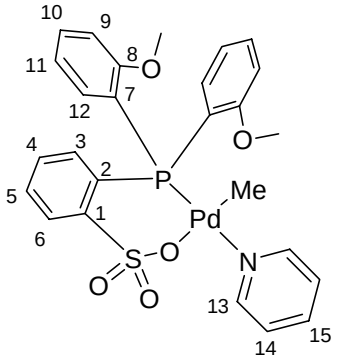

2a-pyr was prepared by modification of a reported procedure.[6] 115 mg (0.20 mmol) of complex **2a-TMEDA** were dispersed in methylene chloride. After addition of 5 equivalents of pyridine, a clear solution formed immediately. After stirring for 60 minutes, the volatiles were removed under reduced pressure to yield 107 mg (0.18 mmol, 89%) of **2a-pyr**. ^1H NMR correspond to previously reported[6] values.

^{1}H NMR (400 MHz, CD_2Cl_2): δ = 8.76 (d, $^{3}J_{HH}$ = 4.6 Hz, $^{4}J_{HH}$ = 1.5, 2H, 13-H), 8.06 (dd, $^{3}J_{HH}$ = 7.5, $^{4}J_{PH}$ = 4.9, 1H, 6-H), 7.88 (tt, $^{3}J_{HH}$ = 7.7, $^{4}J_{HH}$ = 1.5, 1H, 15-H), 7.70 – 7.57 (m br, 2H, 10-H), 7.54 (t, $^{3}J_{HH}$ = 7.8, 2H, 14-H), 7.51 – 7.44 (m, 3H, 5-H and 12-H), 7.30 (m, 2H, 3-H and 4-H), 7.04 (vt, *J* = 7.5, 2H, 11-H), 6.97 (dd, *J* = 8.2, *J* = 4.7, 2H, 9-H), 3.66 (s, 6H, OCH_3), 0.24 (d, $^{3}J_{PH}$ = 2.8, 3H, Pd-CH_3). ^{13}C NMR (101 MHz, CD_2Cl_2) δ = 161.17 (d, $^{2}J_{PC}$ = 2.4, C8), 150.88 (C13), 149.20 (d, $^{2}J_{PC}$ = 15.3, C1), 138.78 (C15), 138.15 (br., C5), 135.24 (C3), 133.74 (C10), 130.66 (C12), 128.96 (d, $^{3}J_{PC}$ = 7.1, C4), 128.04 (d, $^{1}J_{PC}$ = 49.8, C2), 128.01 (d, $^{3}J_{PC}$ = 8.3, C6), 125.62 (s, C14), 121.02 (d, $^{3}J_{PC}$ = 11.8, C11), 116.84 (d, $^{1}J_{PC}$ = 57.3, C7), 111.99 (d, $^{3}J_{PC}$ = 4.6, C9), 55.82 (s, OCH_3), 0.40 (Pd-CH_3). ^{31}P NMR (161.8 MHz, CD_2Cl_2) 21.54.

C. {(κ^2-*P,O*)-2-[Di(2-methoxyphenyl)phosphino]benzenesulphonato} (dimethyl sulfoxide) palladium(II)-methyl (2a-DMSO)

115 mg (0.20 mmol) of **2a-TMEDA** were dispersed in 50 mL of DMSO at room temperature. The solvent was removed under reduced pressure. The dinuclear TMEDA complex is only poorly soluble in DMSO (complete conversion required the complete dissolution of **2a-TMEDA**), therefore this operation was repeated until a homogeneous DMSO solution was obtained. After removal of DMSO under reduced pressure, the resulting solid was dispersed in diethyl ether, and isolated by filtration to yield 90.1 mg (0.15 mmol, 76%) of **2a-DMSO**.

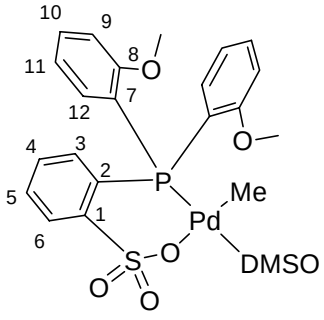

^{1}H-NMR (600 MHz, CD_2Cl_2, 25 °C): δ 8.06 (ddd, $^{3}J_{HH}$ = 8.0 Hz, $^{4}J_{PH}$ = 4.9, $^{4}J_{HH}$ = 1.0, 1H, 6-H), 7.55 (vt, *J* = 7.6, 2H, 10-H), 7.48 (vt, *J* = 7.5, 2H, 12-H), 7.45 (br, 1H, 5-H), 7.31 (vt, *J* = 7.6, 1H, 4-H), 7.25 (ddd, $^{3}J_{HH}$ = 11.3, $^{4}J_{PH}$ = 9.0, $^{4}J_{HH}$ = 1.1, 1H, 3-H), 7.03 (vt, *J* = 7. 5, 2H, 11-H), 6.97 (dd, *J* = 8.4, 2H, 9-H), 3.66 (s, 6H, OCH_3), 2.91 (s, 6H, DMSO), 0.33 (s, Pd-

CH_3). $^{13}C\{^1H\}$ NMR (150 MHz, CD_2Cl_2, 25 °C); δ 161.02 (d, $^2J_{PC}$ = 2.3, C8), 148.75 (d, $^2J_{PC}$ = 15.2, C1), 137.80 (br., C5), 135.16 (d, $^2J_{PC}$ = 1.9, C3), 133.98 (C10), 130.96 (C12), 129.32 (d, $^2J_{PC}$ = 7.4, C4), 128.17 (d, $^3J_{PC}$ = 8.3, C6), 127.70 ($^1J_{PC}$ = 51.2, C2), 121.14 (d, $^3J_{PC}$ = 11.5, C11), 116.15 (d, $^1J_{PC}$ = 57.2, C7), 111.93 (d, $^3J_{PC}$ = 4.1, C9), 55.83 (OCH_3), 41.64 (DMSO), -10.5 (Pd-CH_3). ^{31}P NMR (161.8 MHz, CD_2Cl_2): δ 20 (br).

Anal. Calcd. (%) for $C_{23}H_{27}PdO_6PS_2$: C, 46.00; H, 4.90; Found: C, 45.97; H, 4.53.

D. {(κ^2-*P,O*)-2-[Di(2-methoxyphenyl)phosphino]benzenesulphonato} (dimethyl sulfoxide) nickel(II)-methyl (1a-DMSO)

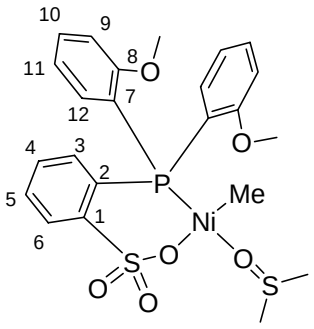

120 mg (0.23 mmol) of **1a-TMEDA** was treated as described for the synthesis of the palladium analogue (**2a-DMSO**) to yield 83 mg (0.15 mmol, 66%) of a yellow solid. Crystals suitable for X-Ray diffraction analysis were grown over two days by diffusion of pentane into a solution of **1a-DMSO** (10 mg) in methylene chloride:dioxane (50:1, 0.5 mL).

NMR (400 MHz, C_6D_6): δ = 8.43 (br. s, 1H, 6-H), 8.23 (dd, *J* = 12.7 Hz, *J* = 8.2, 2H, 12-H), 7.30 (t, *J* = 8.9, 1H, 3-H), 7.11 (t, *J* = 6.9, 2H, 10-H), 7.01 – 6.89 (m, 1H, 5-H), 6.84 – 6.72 (m, 3H, 11 and 4-H), 6.41 (dd, *J* = 7.9, *J* = 4.1, 2H, 9-H), 3.21 (s, 6H, OCH_3), 1.91 (br. S, 6H, DMSO), -0.51 (d, *J* = 5.0, 3H, Ni-CH_3). ^{31}P-NMR (161.8 MHz, C_6D_6, 25°C): δ 15.98.

Anal. Calcd. (%) for $C_{23}H_{27}NiO_6PS_2$: C, 49.83; H, 4.91; Found: C, 49.28; H, 5.10

E. {(κ^2-*P,O*)-[2-di(2-(2',6'-dimethoxyphenyl)phenyl)phosphino] benzenesulphonato} palladium(II) methyl dimethyl sulfoxide (2b-DMSO)

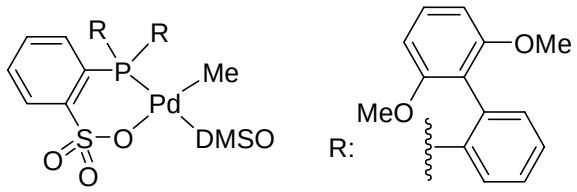

100 mg (0.12 mmol) of **2b-TMEDA** was treated as described for the synthesis of the palladium complex **2a-DMSO** to yield 78 mg (0.10 mmol, 80%) of a off-white solid. Crystals suitable for X-Ray diffraction analysis were grown within 4 d after layering a solution of **2b-DMSO** (5 mg) in methylene chloride (0.1 mL) with pentane (1.5 mL) in an NMR tube.

^{1}H NMR (400 MHz, CD_2Cl_2): δ = 7.71 (m, 3H), 7.46 (vt, *J* = 7.5 Hz, 2H), 7.35 (vt, *J* = 7.7, 2H), 7.30 – 7.21 (m, 1H), 7.16 (vt, *J* = 7.5, 1H), 7.09 (m, 4H), 6.96 (vt, *J* = 7.3, 1H), 6.41 (d, *J* = 8.3, 2H), 6.26 (d, *J* = 8.4, 2H), 3.60 (s, 6H, OCH_3), 3.24 (br. s, 6H, OCH_3), 2.84 (br. s, 6H, DMSO), 0.35 (br. s, 3H, Pd-CH_3). ^{13}C NMR (150 MHz, CD_2Cl_2) δ = 157.96 (C_q, *C*OMe), 157.86 (C_q, Ar-OMe), 148.46 (C_q, d, J_{PC} = 14.7), 141.41 (C_q, d, J_{PC} = 11.0,), 137.35 (CH, d, J_{PC} = 9.8), 135.86 (CH), 134.70 (CH, d, J_{PC} = 8.5), 132.34 (C_q, d, J_{PC} = 54.3), 130.55 (CH), 130.52 (CH), 129.68 (CH), 128.54 (CH), 128.07 (CH, d, J_{PC} = 8.2), 126.96 (CH), 126.60 (CH, d, J_{PC} = 9.8), 118.53 (C_q), 104.27 (CH), 103.52 (CH), 55.81 (s, OCH_3), 55.10 (s, OCH_3), 41.98 (s, DMSO), 5.27 (s, Pd-CH_3). ^{31}P-NMR (161.8 MHz, CD_2Cl_2, 25°C): δ 15.7 br.

III. NMR studies of relative binding of dimethylsulfoxide

An NMR tube was charged with complex **2a-DMSO** (10 mg) and 0.5 mL of CD_2Cl_2. The tube was shaken to form a clear, homogeneous pale yellow solution. Pyridine, 2,6 lutidine or dimethyl-*n*-butylamine, respectively, were added with a gastight syringe. Before and after addition of reagents, ^{1}H and ^{31}P NMR spectra were recorded at 25°C.

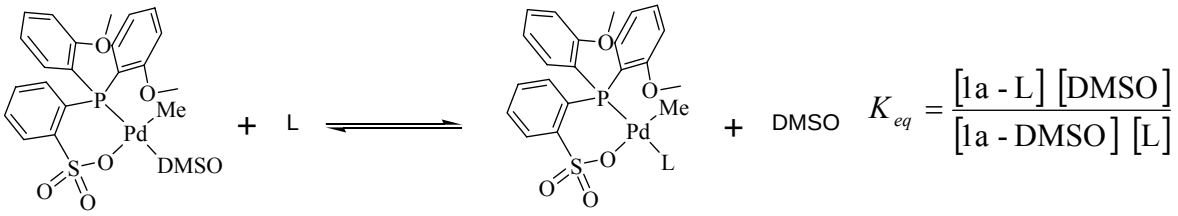

$$K_{eq} = \frac{[1a - L]\,[DMSO]}{[1a - DMSO]\,[L]}$$

In all three cases, DMSO was completely displaced by the respective *N*-donor ligand. This suggests an equilibrium in favor of the corresponding (κ–*N*) complexes, with an equilibrium constant $K_{eq} > 10^2$.

Table S1. Key NMR data of species observed in relative binding studies.

	Pd-CH_3	DMSO	^{31}P	*o*-H of pyridine	NMe_2nBu	2,6 Lutidine
2a-dmso	br. s 0.33	2.91	br. s 20	-	-	-
2a-dmso + 1.4 eq pyridine	d 0.24	2.54	21.51	dd 8.67	-	-
2a-pyr	d 0.24	-	21.54	dd 8.77	-	-
2a-dmso + 1.8 eq DMBA	d 0.03	2.54	22.43	-	t 0.94	-
2a-lut	d -0.04	-	20.4	-	-	3.14
2a-dmso + 1.5 eq 2,6 lutidine	d -0.04	2.54	20.4	-	-	3.14

DMSO in CD_2Cl_2: δ 2.54 ppm; *o*-H of pyridine in CD_2Cl_2: 8.61; $(CH_3)_2N$-$(CH_2)_3$-C***H*****$_3$** in CD_2Cl_2: 0.90; $(C\boldsymbol{H}_3)_2(C_5H_3N)$ in CD_2Cl_2: 2.46

Figure S1. Displacement of DMSO from **2a-dmso** by NMe_2nBu (DMBA).

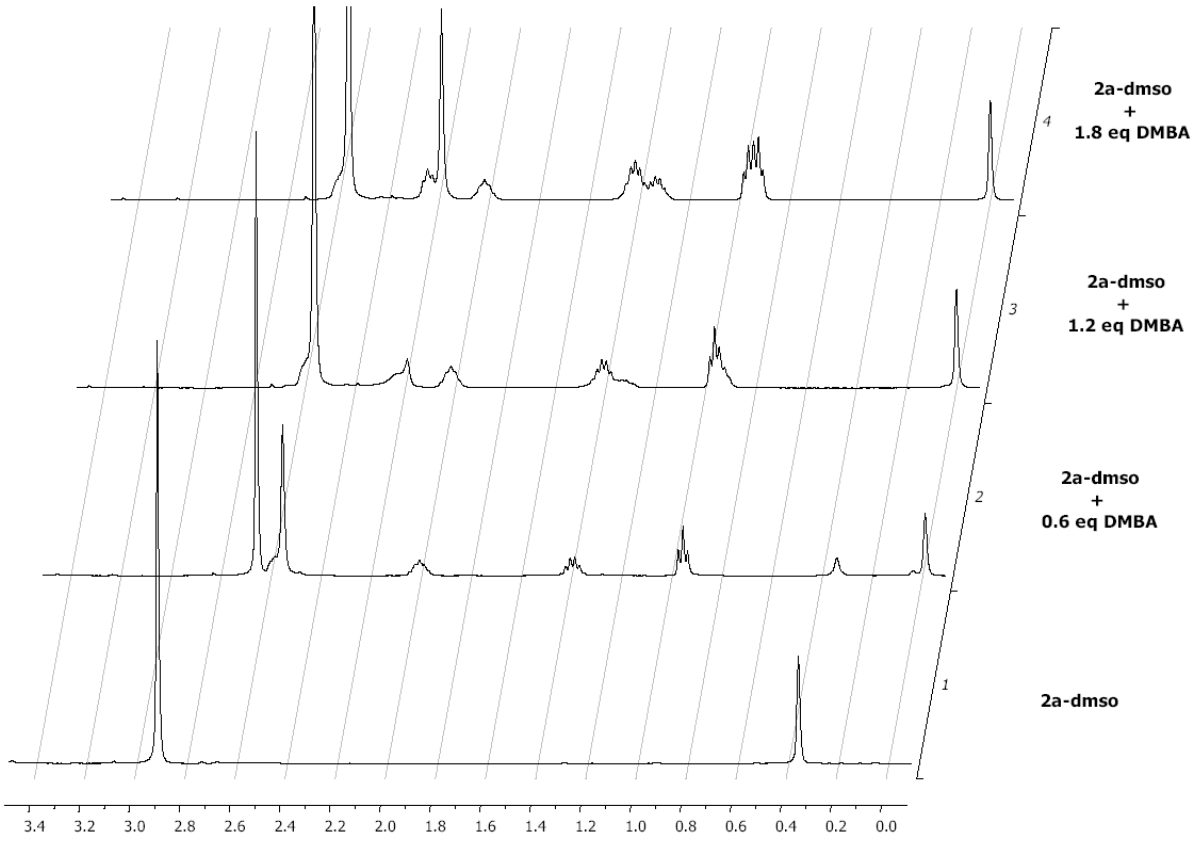

Figure S2. Displacement of DMSO from **2a-dmso** by pyridine.

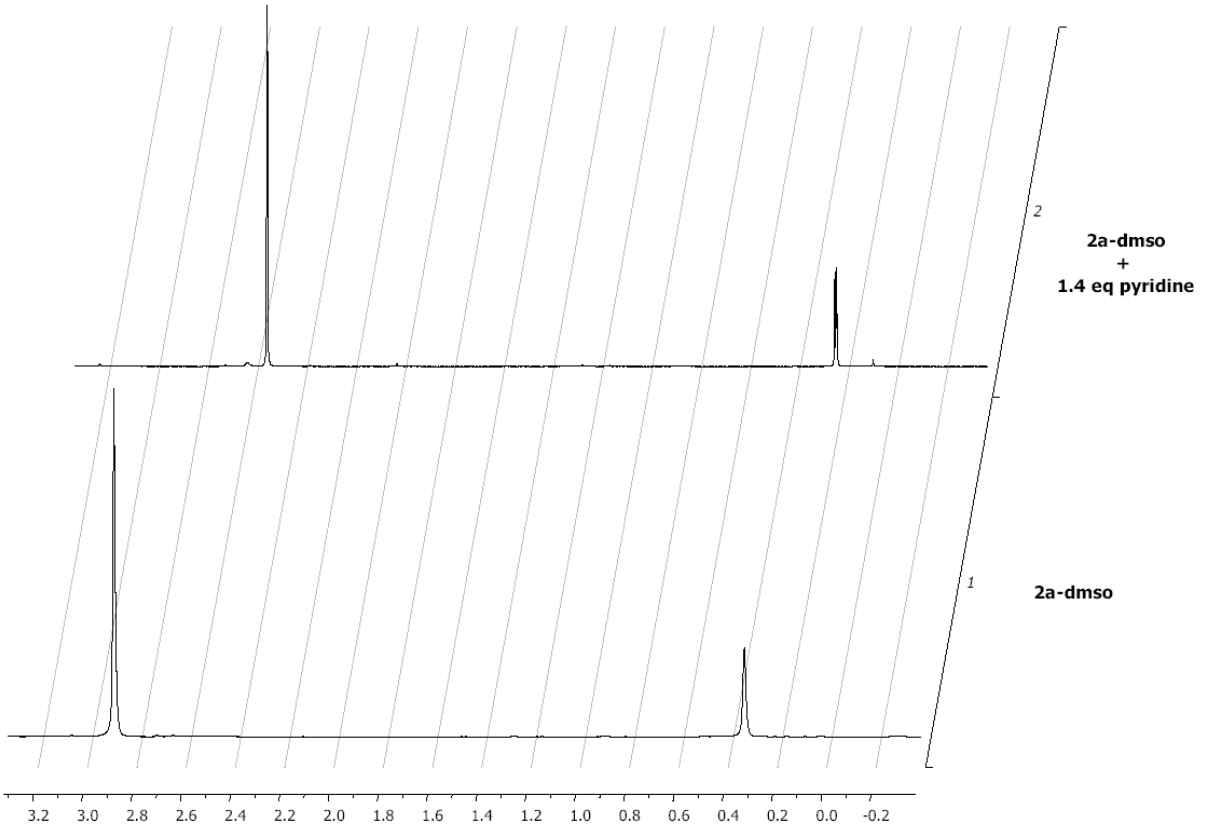

Figure S3. Displacement of DMSO from **2a-dmso** by 2,6-lutidine.

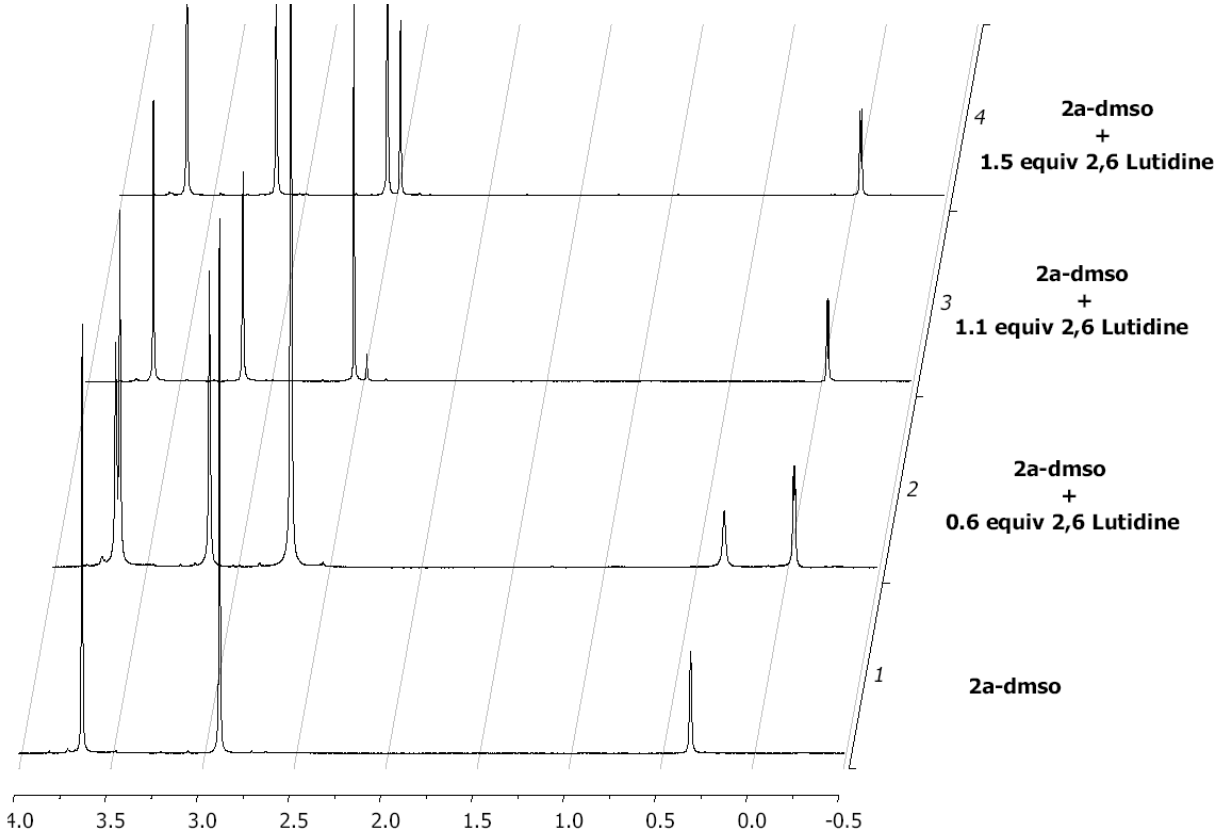

IV. Polymerization and copolymerization of ethylene

A. Homopolymerization of ethylene

Polymerizations were carried out in a 250 mL stainless steel mechanically stirred (750 rpm) pressure reactor equipped with a heating/cooling jacket supplied by a thermostat controlled by a thermocouple dipping into the polymerization mixture. A valve controlled by a pressure transducer allowed for applying and keeping up a constant ethylene pressure. The required flow of ethylene, corresponding to ethylene consumed by polymerization, was monitored by a mass flow meter and recorded digitally. Prior to a polymerization experiment, the reactor was heated under vacuum to the desired reaction temperature for 30 – 60 min and then back-filled with argon.

Standard procedure: A stock solution of the catalyst precursors in methylene chloride containing 1 μmol ml^{-1} was prepared in the drybox, and kept in the refrigerator of the drybox (-30°C). Theses solutions were never stored longer than 12 hours. The reactor was vented, and in a slight argon stream, the solvent was transferred via cannula and the precursor solution was inserted by a syringe to the reactor. The reactor was closed and a constant ethylene pressure was applied. After the desired reaction time the reactor was rapidly vented and cooled to room temperature. The reaction mixture was stirred with an excess volume of methanol. The polymer was isolated by filtration, washed several times with methanol, and dried in vacuo at 50 °C.

These catalysts are highly active single site catalysts and exhibit particular behaviour depending on the reaction medium. In the following part a comparison of the ethylene pressure dependence of the activity of the corresponding DMSO, TMEDA and pyridine complex is presented.

1. Ethylene polymerization with Ni(II) complexes

We recently report the synthesis and the polymerization behaviour of **1a-TMEDA** and **1a-pyridine**.[4] The polymerization behaviour of these complexes by comparison to **1a-DMSO** at different ethylene pressures was studied. Polymerizations were performed in a water cooled

reactor at sufficient low catalyst loading to avoid reaction exotherms greater than 2 °C. This enables a reliable comparison of catalyst activities and lifetimes.

Table S2. Polymerization of ethylene with Ni(II) complexes.

Entry	Precursor	P [bar]	average TOF [mol (C_2H_4) mol (Ni)$^{-1}$ h^{-1}]	Polymer yield [g]	M_n [a] (NMR) [g mol^{-1}]	Branches[b] [/1000C]
2-1	**1a-pyr**	40	5.92×10^5	29.04	1×10^3	17
2-2	**1a-pyr**	30	5.18×10^5	25.38	1×10^3	17
2-3	**1a-pyr**	20	3.76×10^5	18.42	1×10^3	16
2-4	**1a-pyr**	15	1.34×10^5	6.58	1×10^3	14
2-5	**1a-TMEDA**	40	4.15×10^5	20.35	1×10^3	17
2-6	**1a-TMEDA**	30	2.92×10^5	14.34	1×10^3	17
2-7	**1a-TMEDA**	20	2.70×10^5	13.25	1×10^3	17
2-8	**1a-TMEDA**	15	9.98×10^4	4.89	1×10^3	15
2-9	**1a-DMSO**	40	7.75×10^5	37.96	1×10^3	17
2-10	**1a-DMSO**	30	7.74×10^5	37.92	1×10^3	17
2-11	**1a-DMSO**	20	4.54×10^5	22.25	1×10^3	17
2-12	**1a-DMSO**	15	3.63×10^5	17.79	1×10^3	16

Reaction conditions: 100 mL of toluene; 70 °C; 3.5 µmol of Ni(II); 30 min polymerization time. [a] Determined by ^{1}H NMR at 130°C, from integrals of olefinic endgroups. [b] Determined by ^{13}C NMR at 130°C, methyl branches observed exclusively.

1a-dmso is a single component precursor catalyst for ethylene polymerization (Table S2). With an average activity approaching 10^6 TO h^{-1} (TO = mol olefin converted per mol of metal present in the reaction mixture) in a half hour polymerization experiment (entry 2-9), **1a-dmso** is amongst the most active and productive neutral Ni(II) catalysts reported for ethylene polymerization or oligomerization to date.[4] Low molecular weight moderately branched material is formed. The activity observed for **1a-dmso** exceeds that of the analogous *N*-coordinated pyridine complex **1a-pyr** and the tertiary amine complex **1a-tmeda**, particularly at a low ethylene pressure.

2. Ethylene polymerization with 2b-DMSO.

Due to an extremely high reactivity of the catalyst, it was difficult to control the exothermicity of polymerization. Therefore, polymerizations were performed at 70 °C, even though higher activity could be observed at higher temperature.

Polymer yields increase with ethylene pressure (2 to 7.5 bar), but level off above ca. 7.5 bar (Table S3). Observed molecular weights increase between 2 to 7.5 bar and are constant at higher pressure. In contrast to **2a-DMSO**, strictly linear high molecular weight material was obtained even at low ethylene pressure.

Table S3. Ethylene polymerization with **2b-DMSO**.

Entry	Pd [μmol]	T [°C]	Time [min]	P [bar]	average TOF [mol (C_2H_4) mol (Pd)$^{-1}$ h^{-1}]	Polymer yield [g]	M_n [a] [g mol^{-1}]	M_w/M_n [a]	Branches [b] [/1000C]
3-1	3.5	80 to 95	10	10	5.75×10^5	9.39	50×10^3	2.0	<1
3-2	2	70	30	15	1.86×10^5	5.19	250×10^3	1.6	<1
3-3	2	70	30	10	1.82×10^5	5.06	210×10^3	1.7	nd
3-4	2	70	30	7.5	1.81×10^5	4.91	200×10^3	1.6	nd
3-5	2	70	30	5	1.34×10^5	3.74	130×10^3	1.6	nd
3-6	2	70	30	2	5.36×10^4	1.50	80×10^3	1.8	<1
3-7	1	95	30	20	9.94×10^5	13.67	47×10^3	2.7	<1

Reaction conditions: 100 mL of toluene (entry 3-7: 150 mL); 30 min polymerization time. [a] Determined by GPC at 160°C, referenced to linear PE standards. [b] Determined by ^{13}C NMR at 130°C.

3. Ethylene polymerization with 2a-lut

Ethylene pressure dependence was investigated as well for **2a-lut**. Polymer yields increase with ethylene pressure in the range investigated, up to 15 bar (Table S4).

Table S4. Ethylene polymerization with **2a-lut**.

Entry	P [bar]	average TOF [mol (C_2H_4) mol (Pd)$^{-1}$ h^{-1}]	Polymer yield [g]
4-1	2	2.4×10^4	1.16
4-2	5	3.6×10^4	1.77
4-3	7.5	4.9×10^4	2.40
4-4	10	5.5×10^4	2.68
4-5	15	6.5×10^4	3.17

Reaction conditions: 100 mL of toluene; 80 °C, 3.5 μmol of Pd(II); 30 min polymerization time.

B. Ethylene-methyl acrylate copolymerization.

An identical procedure as for ethylene homopolymerization was applied to copolymerization with methyl acrylate (MA). The solution of toluene and MA (with a total volume of 50 mL) was cannula transfered into the reactor under an argon counter stream. The catalyst precursor was dissolved in dichloromethane (1 mL) and inserted by a syringe to the reactor. In order to prevent any radical homopolymerization of methyl acrylate, the radical inhibitor 3,5-Di-*t*-butyl-4-hydroxy-toluene (BHT) was added to the reaction mixture.

In order to prevent loss of any oligomeric material, the polymer was not precipitated. Toluene and comonomer were removed under vacuum, and the residue was dried in vacuo at 50 °C for several days. Polymer samples with MA-contents above 25 mol% MA were

dissolved in diethyl ether and filtrated over celite, in order to remove residual ligand and also palladium black, formed in some experiments.

V. Homooligomerization of methyl acrylate

An 8 mL screw-cap vial was charged with 5 mL of an MA solution in toluene (4 mol L^{-1}), 125 mg of BHT, and 48 mg (80 µmol) of **2a-DMSO**. The mixture was stirred at 95°C for 4 hours. After the desired reaction time, decomposed catalyst was removed by filtration over celite. Unreacted monomers and solvent were removed in vacuuo. The resulting liquid was dissolved in diethyl ether and filtrated over silica, yielding 820 mg of a transparent viscous liquid (which still contains the initial 120 mg BHT).

In parallel, a control experiment was carried out. 5 mL of MA solution in toluene (4 mol L^{-1}), 125 mg of BHT and 10 mg (78 µmol) of DMSO were stirred at 95°C. After 4 hours, all volatiles were removed under vacuum yielding a white powder (128 mg). This powder was characterized by NMR and assigned to be pure BHT.

The above catalytic MA oligomerization was also carried out in the absence of BHT. Essentially the same amount of oligomer, and the same oligomer molecular weight were observed; in addition some high molecular weight poly(methyl acrylate) was formed, presumably via free radical polymerization.

The oligomers were characterized by NMR and mass spectrometry (FAB). Oligomers up to heptamers were detected in the mass spectra (Figure S4; $m/z = n \times 86 + {}^{23}Na$). Olefin end groups formed by β-H elimination were assigned by ^{1}H and ^{13}C NMR. Further analysis revealed that 2,1 insertion modus is predominant but 1,2 insertion were clearly also detected. The majors products were formed from the insertion of methyl acrylate into a palladium hydride bound, however products from insertion into the Pd-Me inititating group of the catalyst precursor were also detected by ^{1}H NMR (δ 1.17 ppm).

Figure S4. FAB spectra of MA-oligomers.

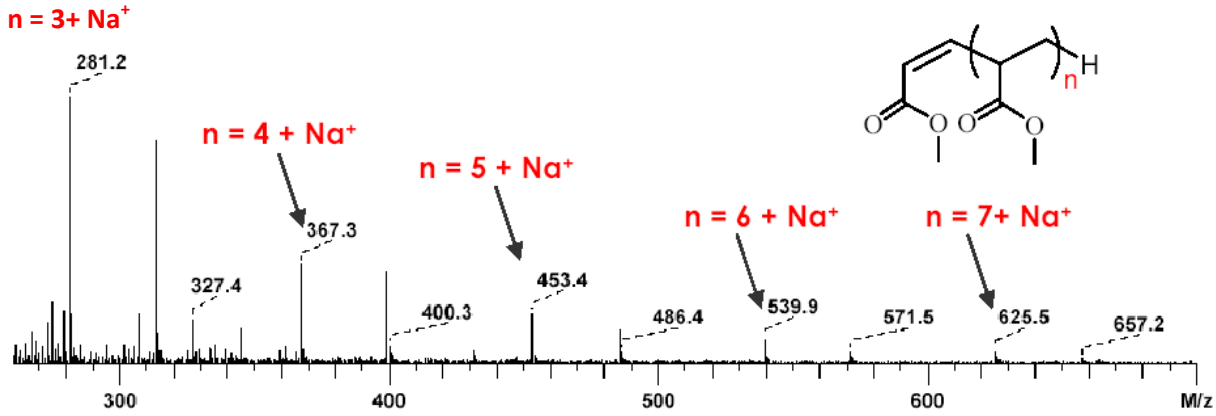

For assignment of the NMR spectra of the oligomers, the raw product was separated by column chromatography over silica gel with a mixture of petrol ether and diethyl ether (80/20 v/v) as eluent. Four different fraction were collected, which were characterized by NMR. Spectra of the higher molecular weight fraction are shown in Figures S5 to S9. The olefin has been isomerized during chromatography leading to the formation of a quaternary carbon (no cross peak on the gHSQC, Figure S9). In this fraction, exclusively 2,1 insertion is observed. A number average degree of polymerization DP_n = ca. 5 was estimated by NMR (Figure S5).

Figure S5

^{1}H NMR of a high M_w oligmer fraction

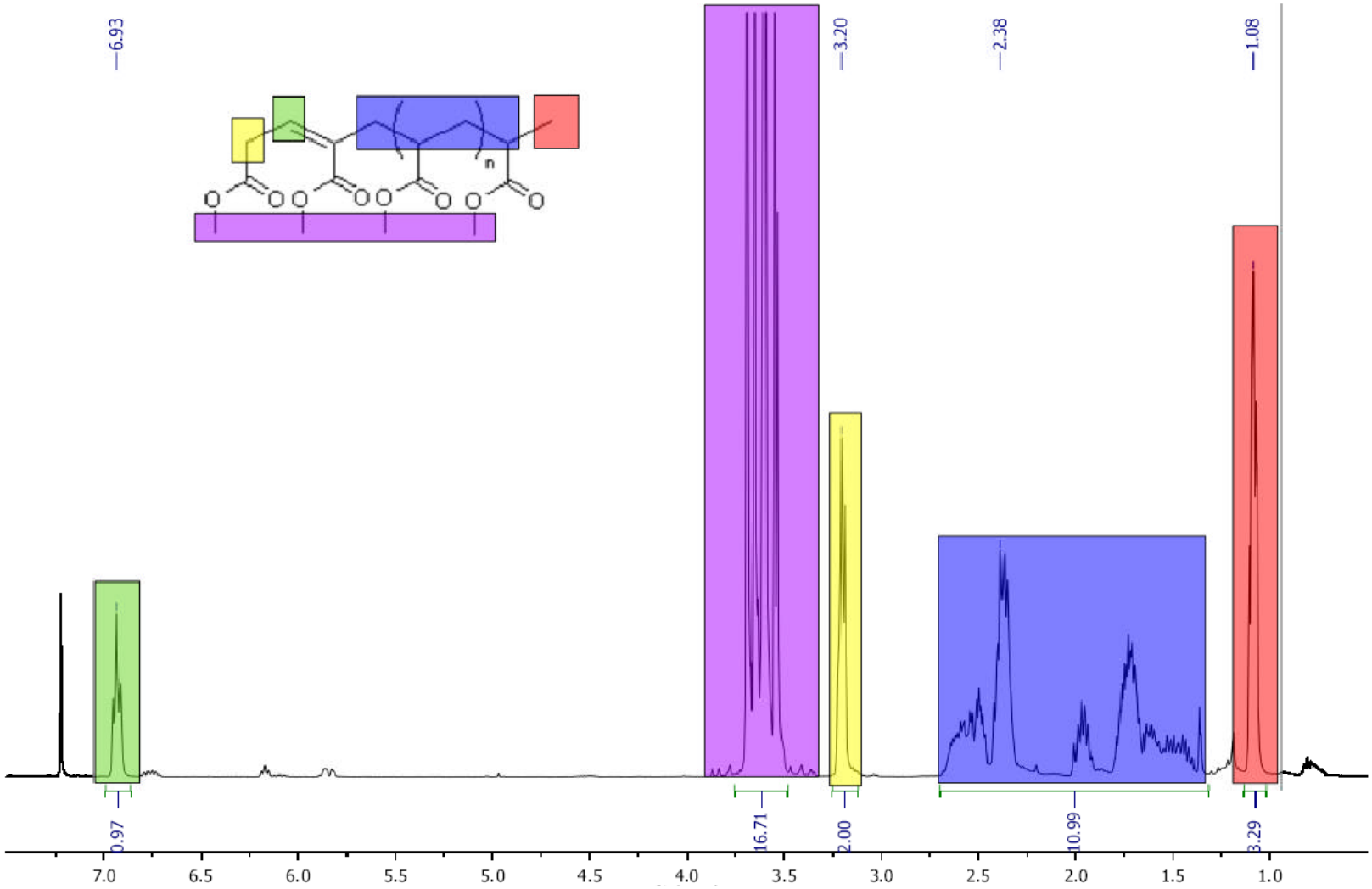

Figure S6

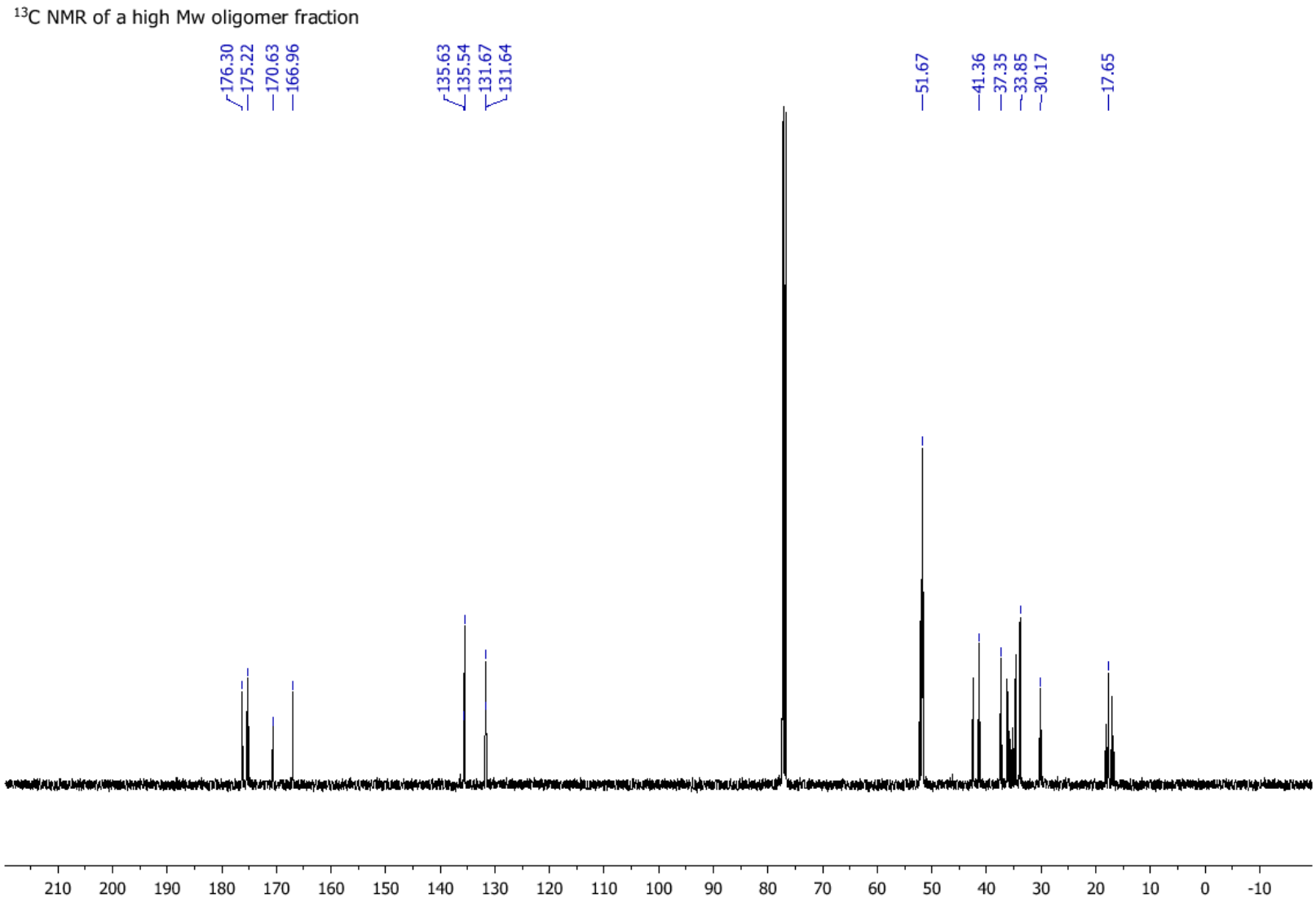
^{13}C NMR of a high Mw oligomer fraction
176.30
175.22
170.63
166.96
135.63
135.54
131.67
131.64
51.67
41.36
37.35
33.85
30.17
17.65
210 200 190 180 170 160 150 140 130 120 110 100 90 80 70 60 50 40 30 20 10 0 -10

Figure S7

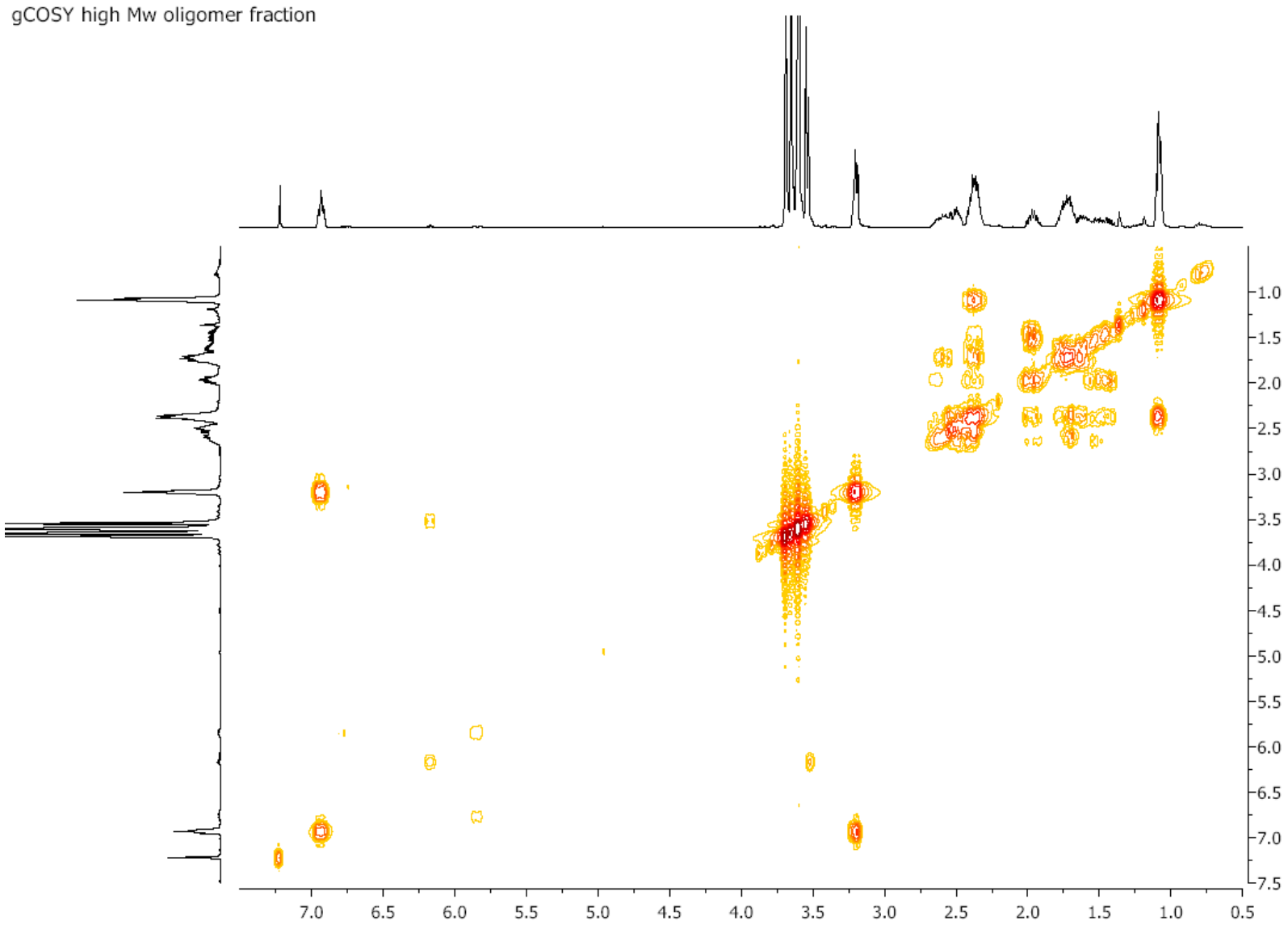
gCOSY high Mw oligomer fraction
7.0
6.5
6.0
5.5
5.0
4.5
4.0
3.5
3.0
2.5
2.0
1.5
1.0
0.5
1.0
1.5
2.0
2.5
3.0
3.5
4.0
4.5
5.0
5.5
6.0
6.5
7.0
7.5

Figure S8

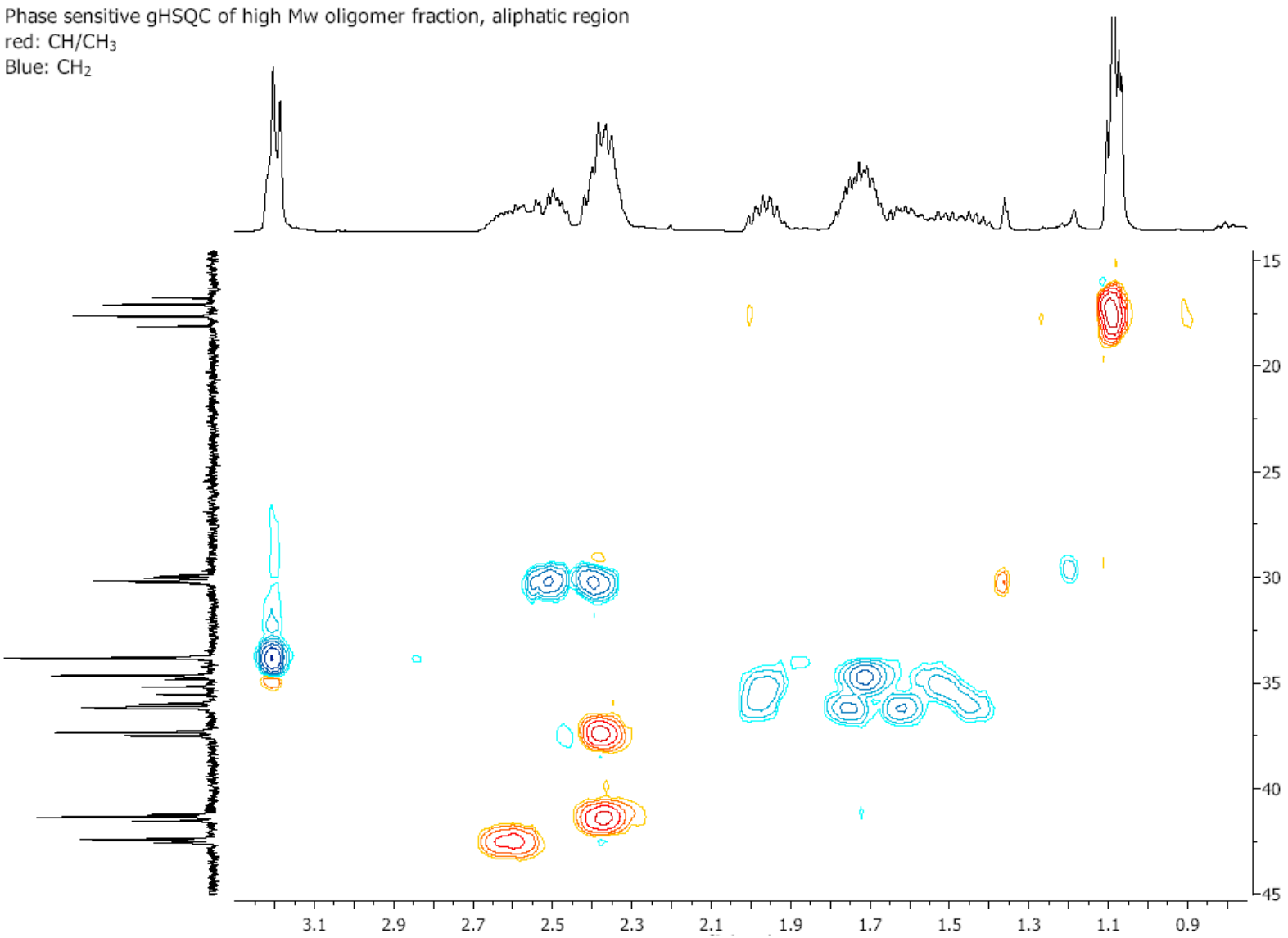
Phase sensitive gHSQC of high Mw oligomer fraction, aliphatic region
red: CH/CH3
Blue: CH2
15
20
25
30
35
40
45
3.1
2.9
2.7
2.5
2.3
2.1
1.9
1.7
1.5
1.3
1.1
0.9

Figure S9

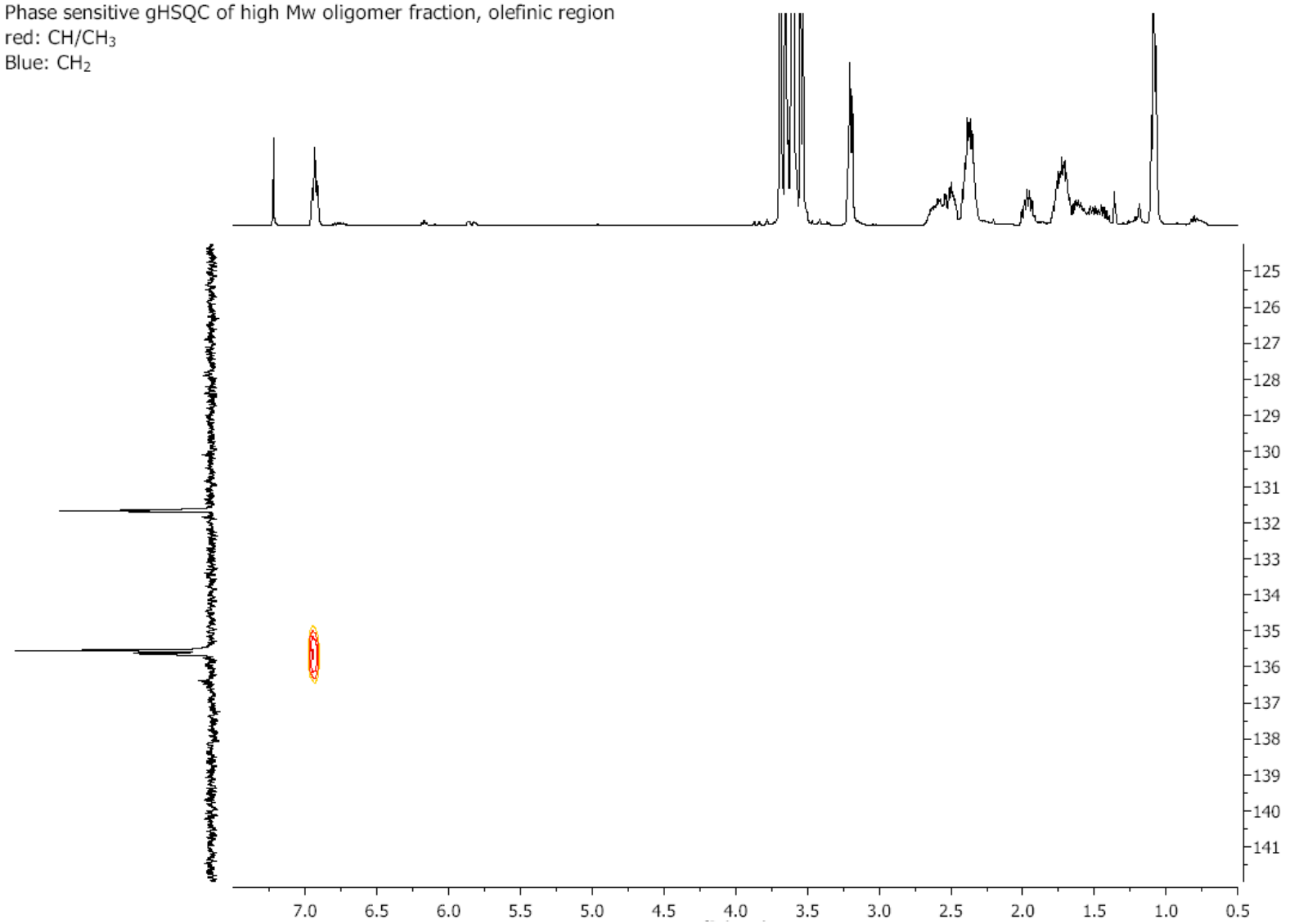
Phase sensitive gHSQC of high Mw oligomer fraction, olefinic region
red: CH/CH3
Blue: CH2
125
126
127
128
129
130
131
132
133
134
135
136
137
138
139
140
141
7.0
6.5
6.0
5.5
5.0
4.5
4.0
3.5
3.0
2.5
2.0
1.5
1.0
0.5

VI. Synthesis of [(P^O)Pd{CH(COOMe)CH_2CH_3}(DMSO)]

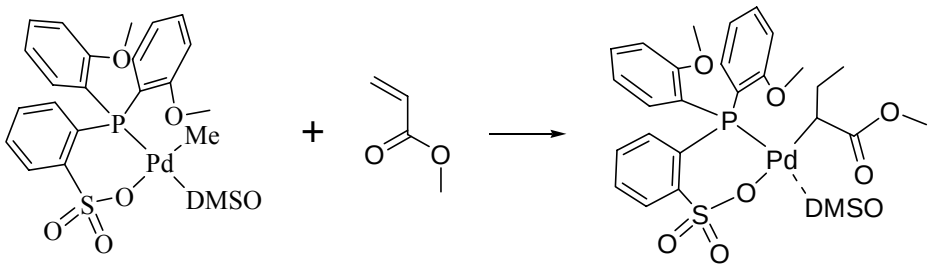

100 mg (0.167 mmol) of **2a-dmso** and 100 equiv. of methyl acrylate were dissolved in methylene chloride. The reaction mixture was stirred for 2 h at room temperature. The volatiles were removed under reduced pressure. The solid was dissolved in THF and filtrated through a syringe filter at low temperature. The solvent was removed in vacuo, and the residual solid was washed with diethyl ether to yield 65 mg of a yellowish powder.

The chemical shift of the DMSO signal does not correspond to free DMSO (free DMSO δ 2.54, observed δ 2.83), and moreover the chemical shift of the carbonyl corresponds to free carbonyl (δ 177.69).[7] Addition of pyridine to **2a-dmso** resulted in the release of free dmso, and formation of the corresponding pyridine complex (vide supra) which is stable at room temperature.

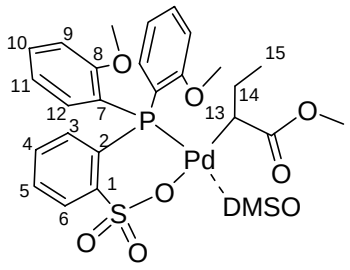

^{1}H NMR (400 MHz, CD_2Cl_2) δ = 8.91 (br. s, 1H), 7.92 (m, *J* = 8.8, 1H), 7.59 (vt, *J* = 7.5, 1H), 7.54 (vt, *J* = 8.1, 1H), 7.42 (m, 2H), 7.29 (vt, *J* = 7.5, 1H),7.19 (m, 2H), 6.99 (m, 2H), 6.85 (dd, *J* = 8.0, *J* = 4.2, 1H), 3.63 (s, 3H, OCH_3), 3.53 (s, 3H, OCH_3), 3.42 (s, 3H, $COOCH_3$), 2.83 (br. s, 6H, DMSO), 1.56 (vt, *J* = 8.6, 1H, 13-H), 1.37 (m, 1H, 14-H), 0.58 (m, 1H, 14-H), 0.09 (t, *J* = 6.6, 3H, 15-H). ^{13}C NMR (101 MHz, CD_2Cl_2) δ = 177.69 (d, *J* = 2.4 Hz, *C*$OOCH_3$), 160.41 + 159.77 (d each, *J* = 2.1 + 4.0, C8 + C8'), 146.82 (d, *J* = 14.6, C1), 144.83 – 143.21 (br, C5), 135.06 (d, *J* = 2.1, C3), 134.71 + 133.44 (s each, C10 and C10'), 130.31 (d, *J* = 2.2, C12 or C12'), 128.34 (d, *J* = 7.7, C4), 127.01 (d, *J* = 8.6, C6), 126.06 (d, *J* = 54.7, C2), 120.49 + 120.10 (d each, *J* = 10.2 + 16.0, C11 + C11'), 113.92 + 112.64 (d each , *J* = 61.8 + 56.9, C7 + C7'), 111.25 + 110.67 (d each, *J* = 5.0 + 3.8, C9 + C9'), 55.69 + 54.73

(s each, OCH_3), 51.06 (s, $COOCH_3$), 39.58 (br. s, DMSO), 31.67 (s, C13), 22.09 (s, C14), 13.52 (d, J = 4.7, C15). ^{31}P NMR (161.8 MHz, CD_2Cl_2, 25°C): δ 25.6 br.

VII. Characterization of ethylene-methyl acrylate copolymer

GPC traces confirmed the absence of any radically polymerized methyl acrylate homopolymer. This is also evident from the NMR spectra of the copolymers.

Analysis of end groups by NMR reveals that β-H elimination occurred preferentially after methyl acrylate insertion. An increase of methyl acrylate content in the polymer lead to a decrease of terminal olefin end groups. End groups corresponding to β-H elimination after at least 2 consecutive acrylate insertions were unambiguously assigned. 2,1-insertion of methyl acrylate into a Pd-H bond is the main mode of chain initiation at high MA concentration.

For the assignment of copolymers with MA-contents below 25 mol-%, cf. [8]; for copolymers from radical polymerization with an acrylate incorporation of > 50 mol-% cf. [9].

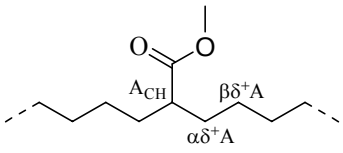

Random

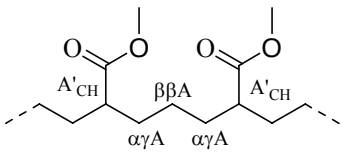

Alternating

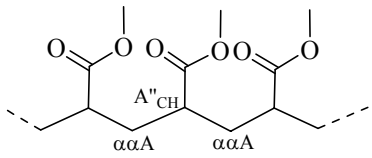

Consecutive acrylate insertion

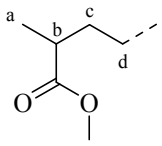

Product of insertion of MA on Pd hydride

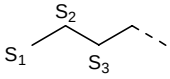

Product of insertion of ethylene on Pd methyl or hydride

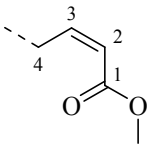

Product of ß-H elimination after acrylate insertion

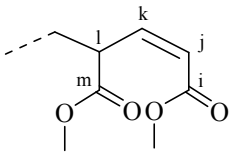

Product of ß-H elimination after consecutive acrylate insertion

Figure S10. ^{1}H NMR spectrum of ethylene-methyl acrylate copolymer with 52 mol-% incorporation of acrylate (entry 2-5).

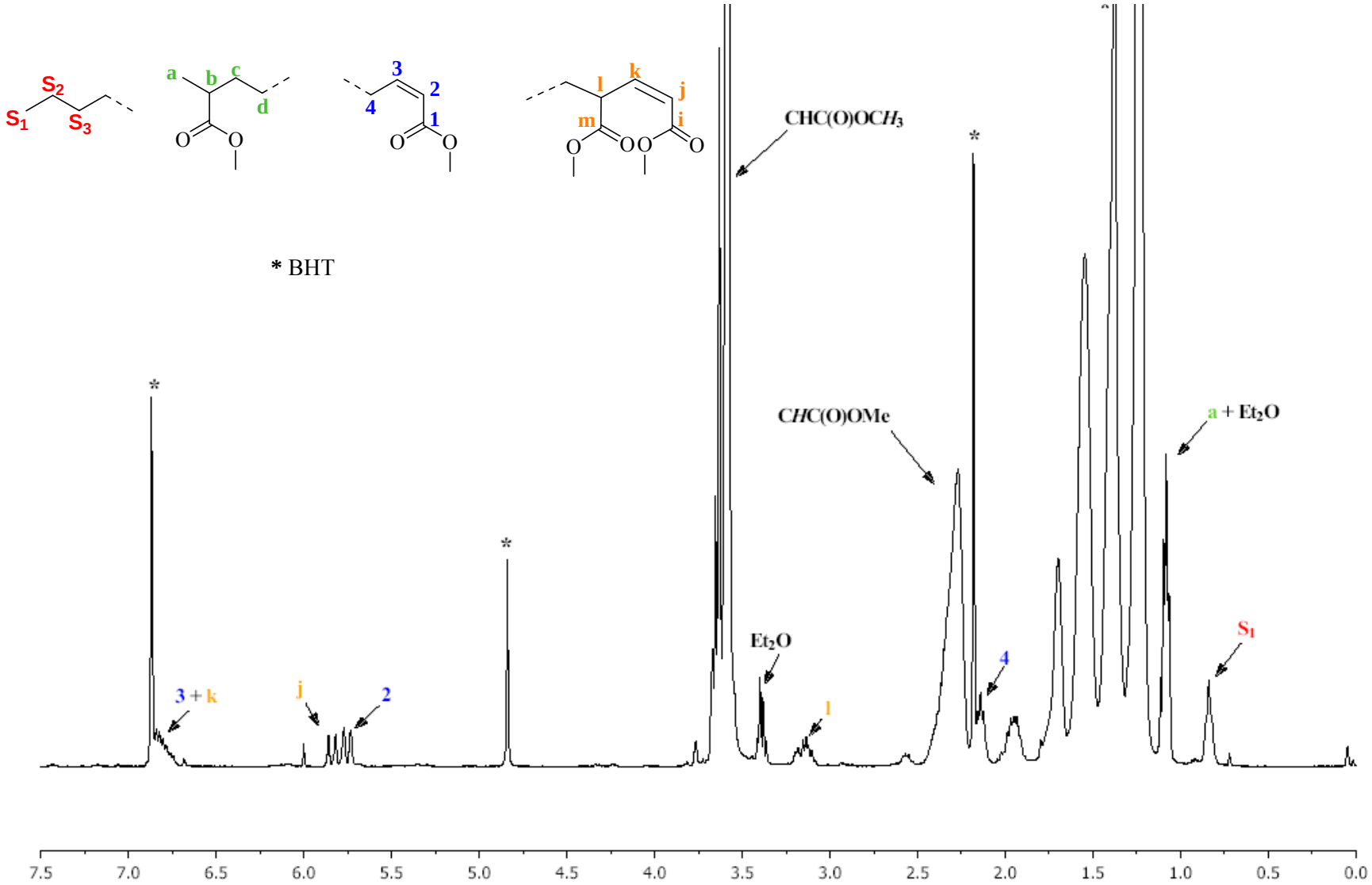

Figure S11. ^{1}H NMR spectrum of ethylene-methyl acrylate copolymer with 35 mol-% acrylate incorporation (entry 2-4).

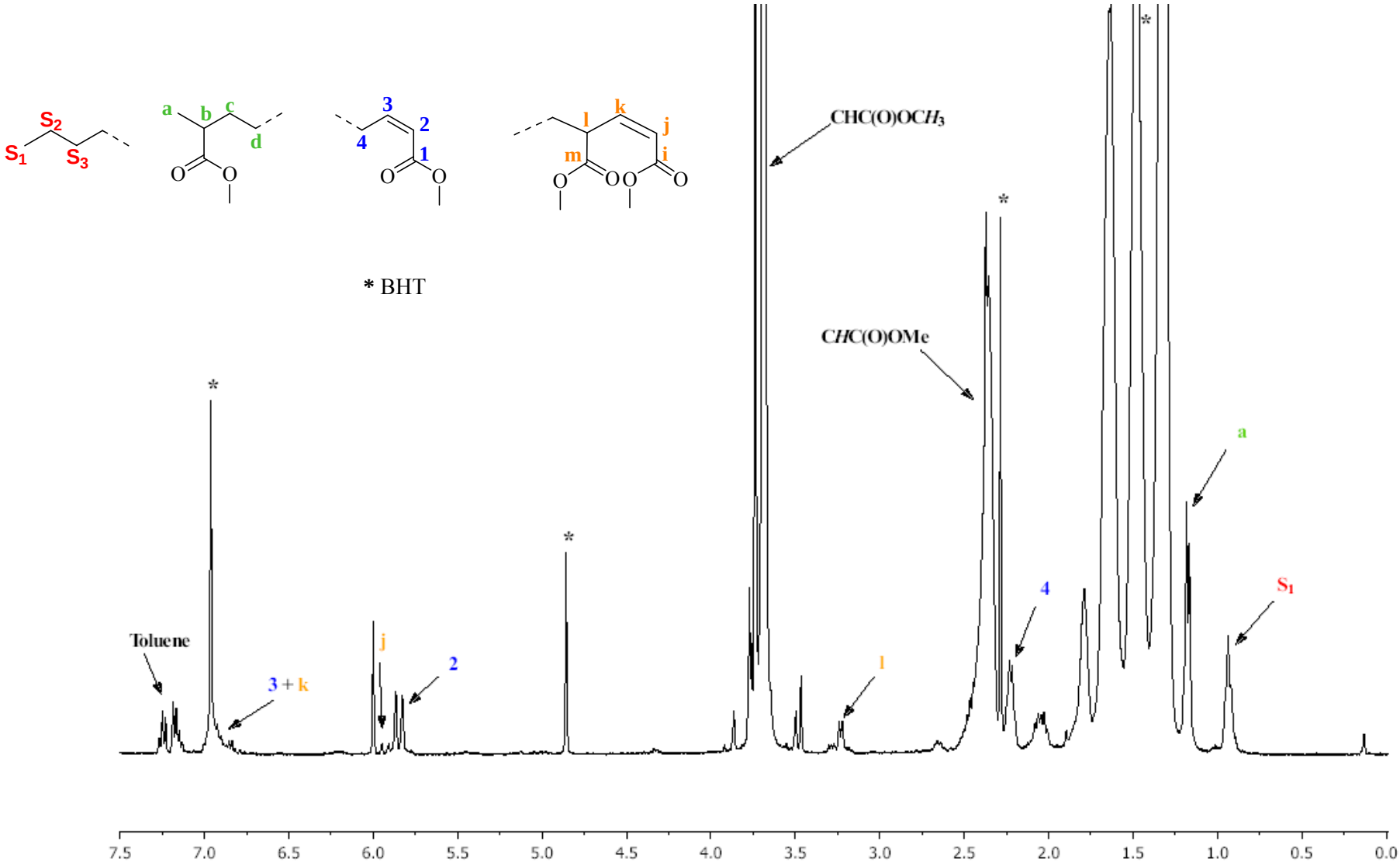

Figure S12. ^{1}H NMR spectrum of methyl acrylate homopolymer from comparative free radical polymerization experiment (M_n = 110 000 g mol^{-1})

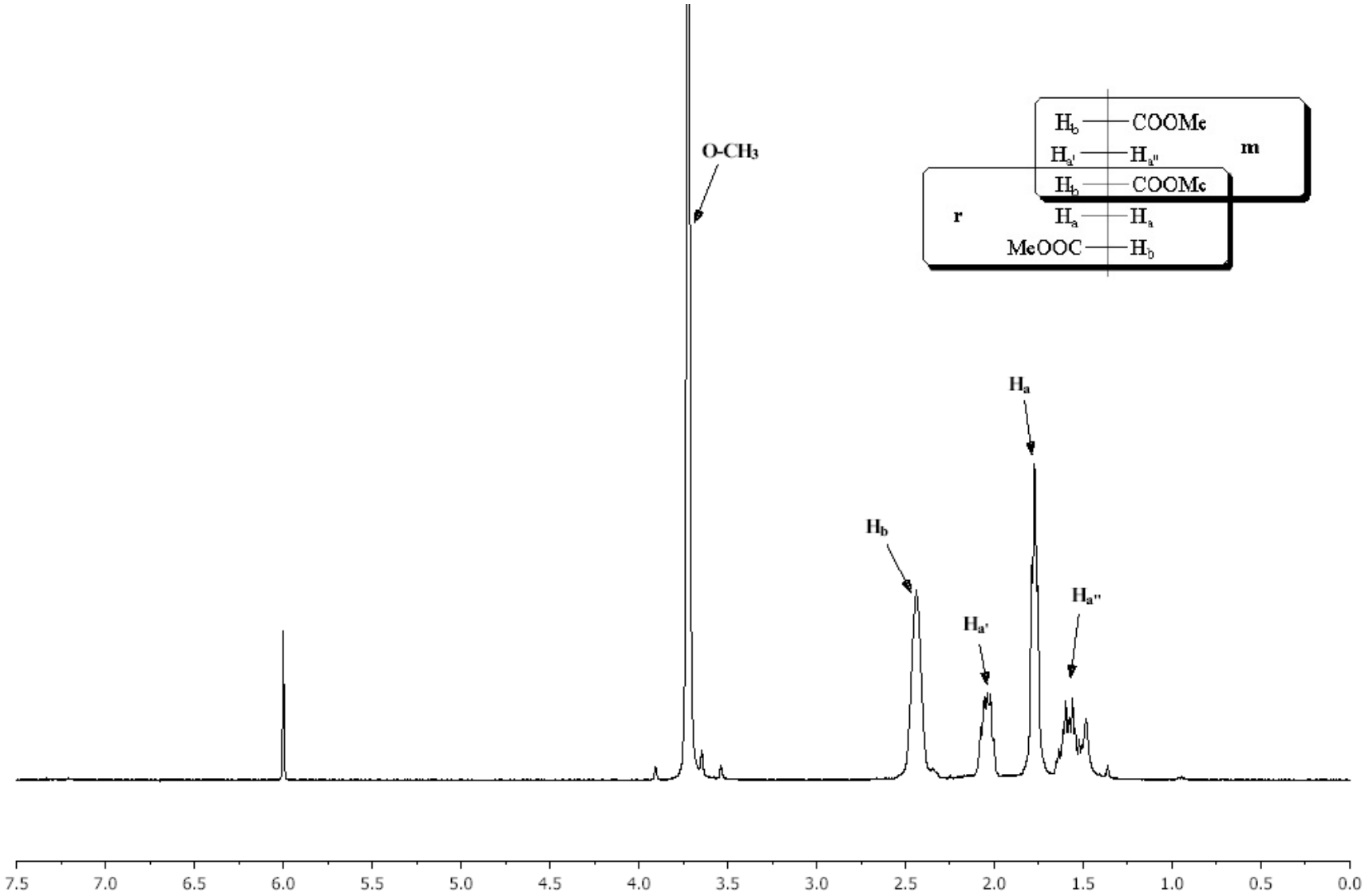

Figure S13. ^{1}H NMR spectra of poly(methyl acrylate) from radical polymerization (red) and copolymer with 52 mol-% incorporation (black)

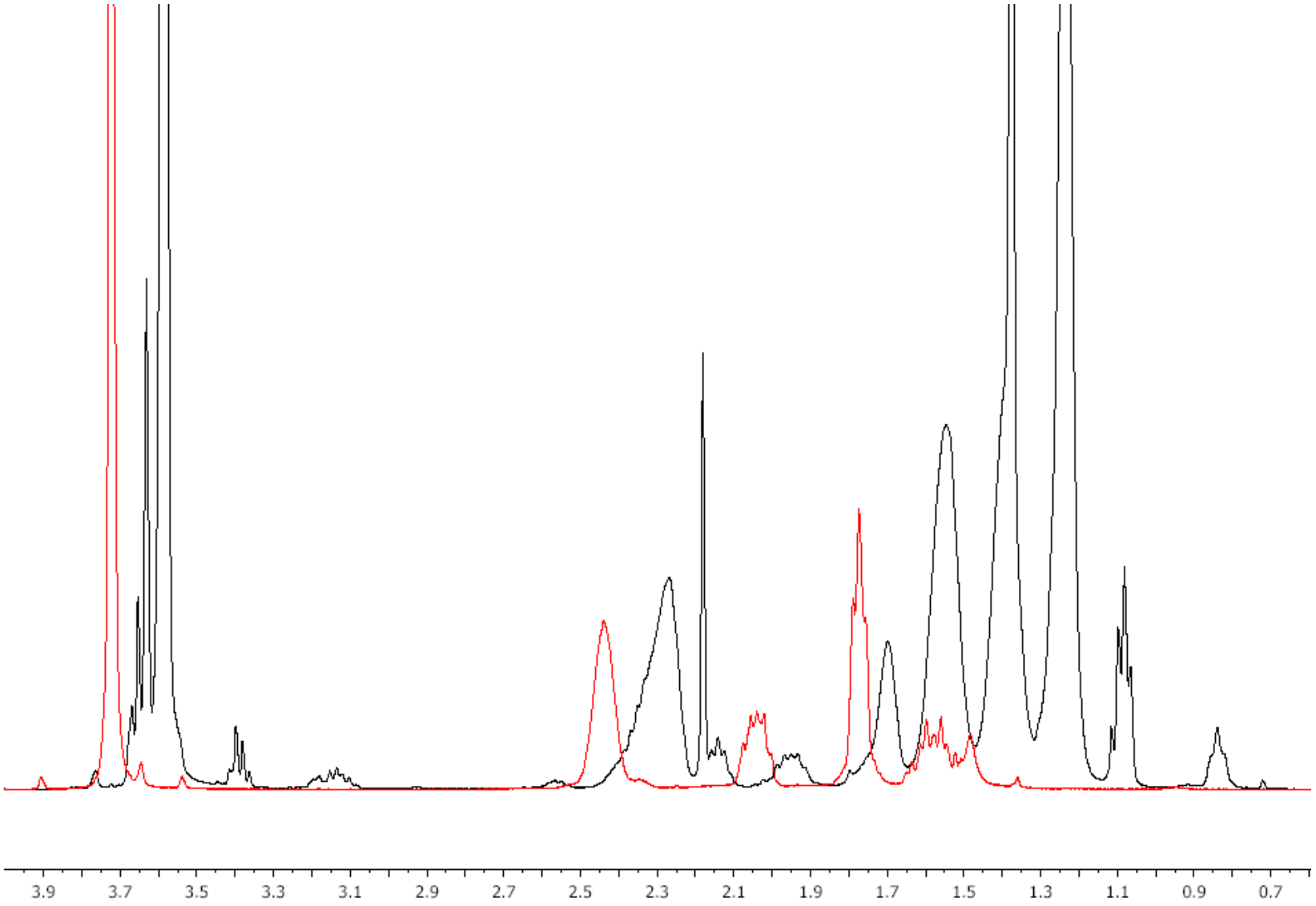

Figure S14. ^{13}C NMR spectrum of ethylene-methyl acrylate copolymer with 52 mol-% incorporation, aliphatic region

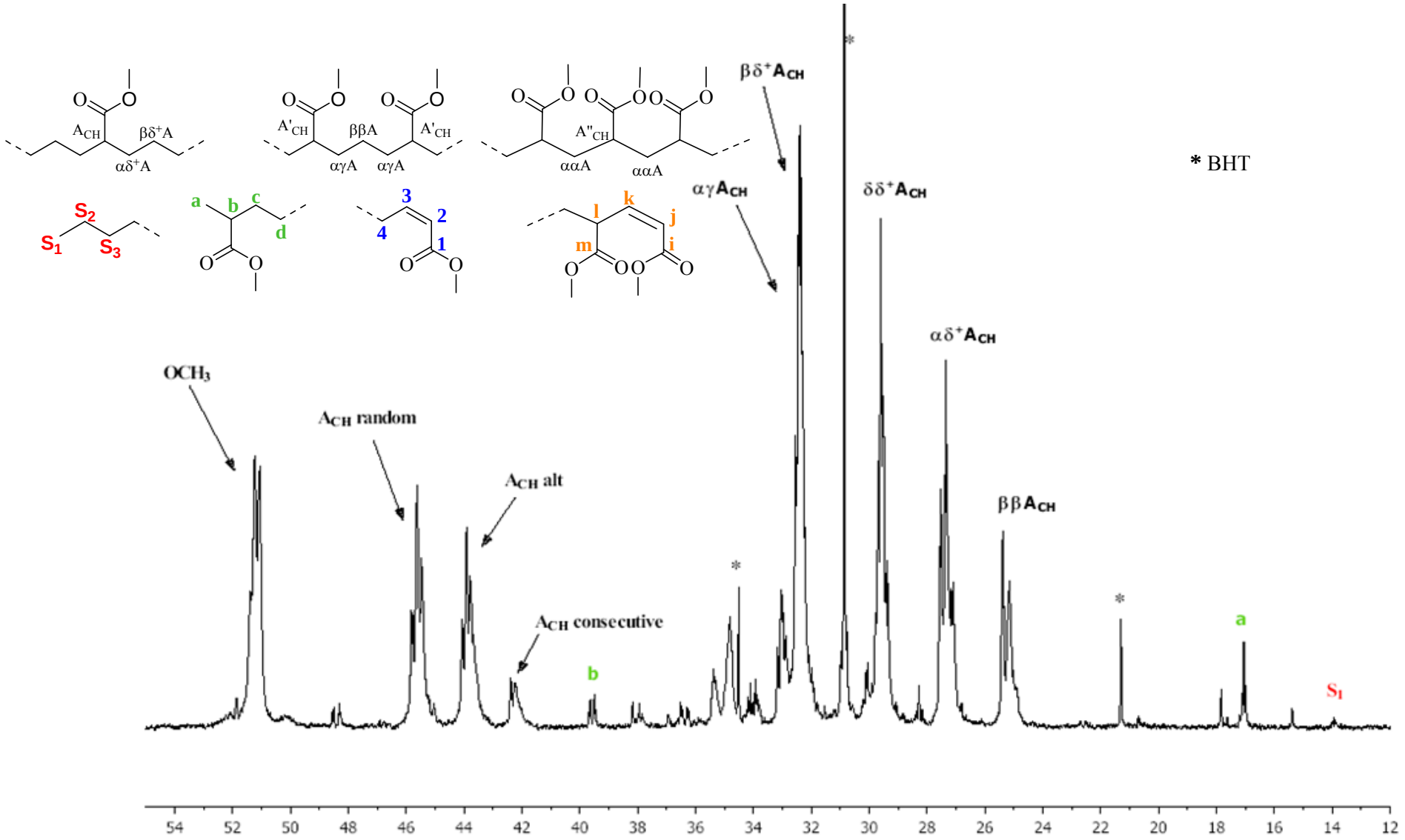

Figure S15. ^{13}C NMR spectrum of ethylene-methyl acrylate copolymer with 52 mol-% acrylate incorporation, olefinic region

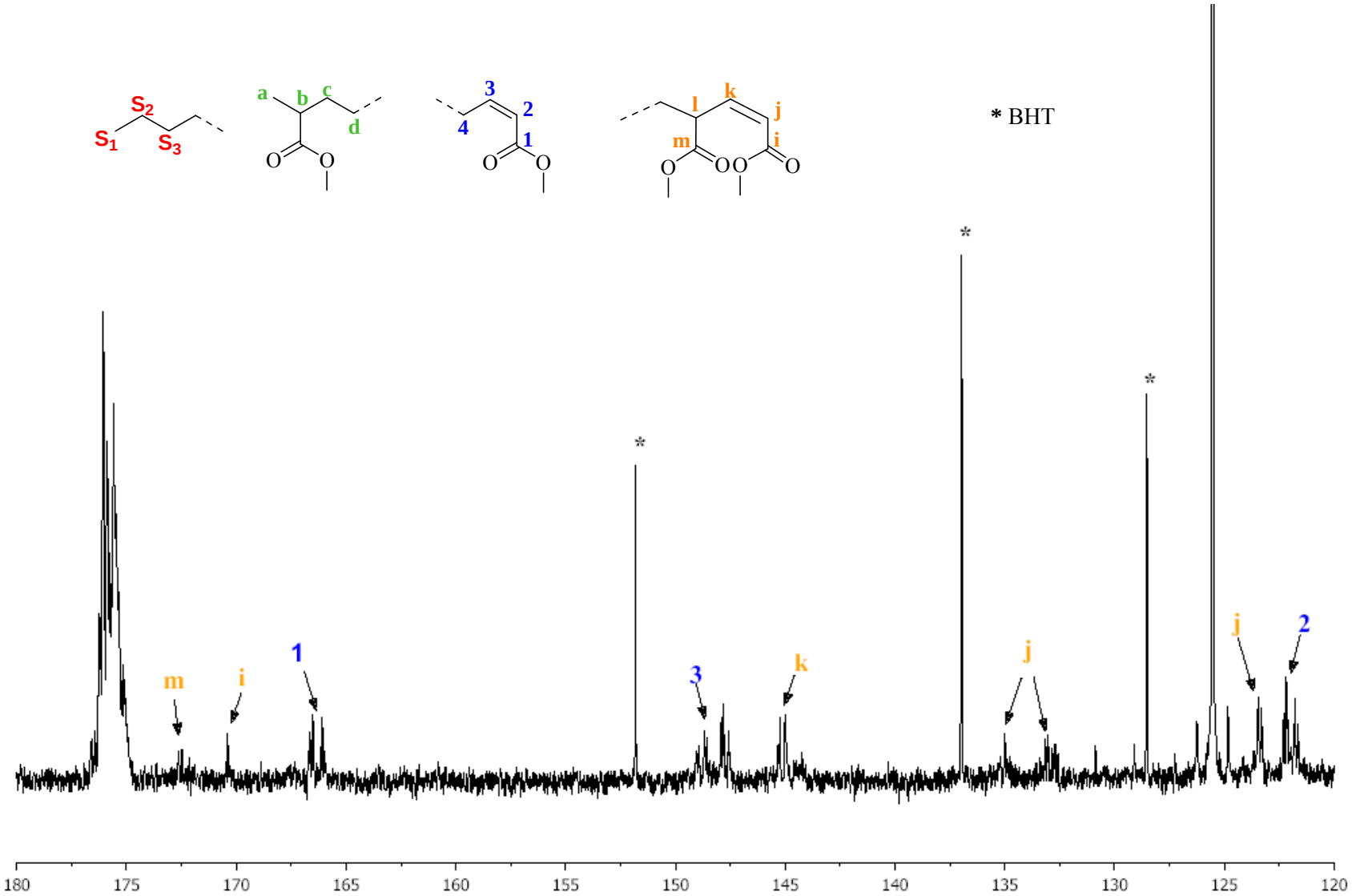

Figure S16. ^{13}C NMR spectrum of methyl acrylate homopolymer from free radical polymerization (M_n = 110 000 g mol^{-1})

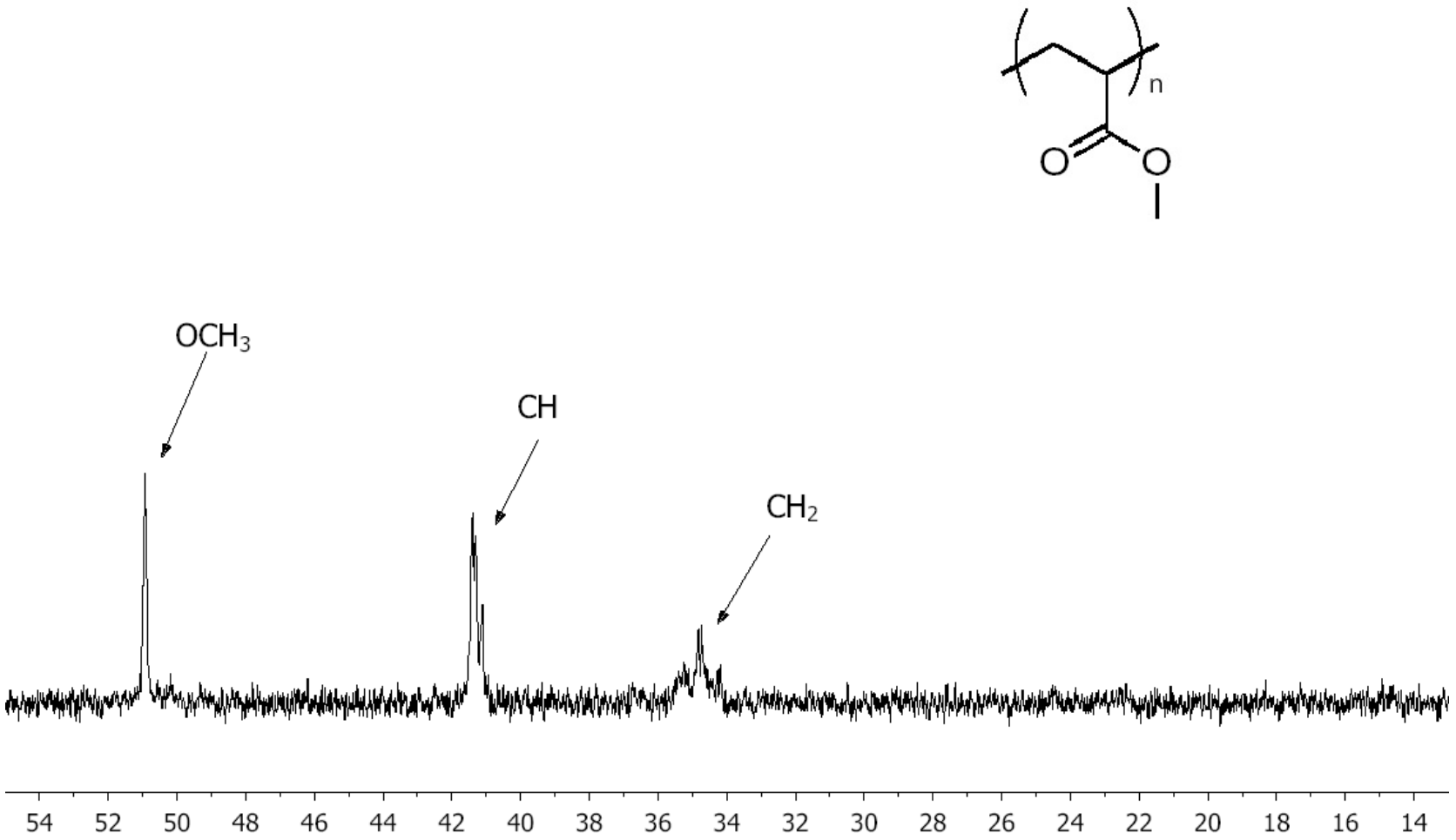

Figure S17. ^{13}C NMR spectra of poly(methyl acrylate) from radical polymerization (red) and copolymer with 52 mol-% incorporation (black)

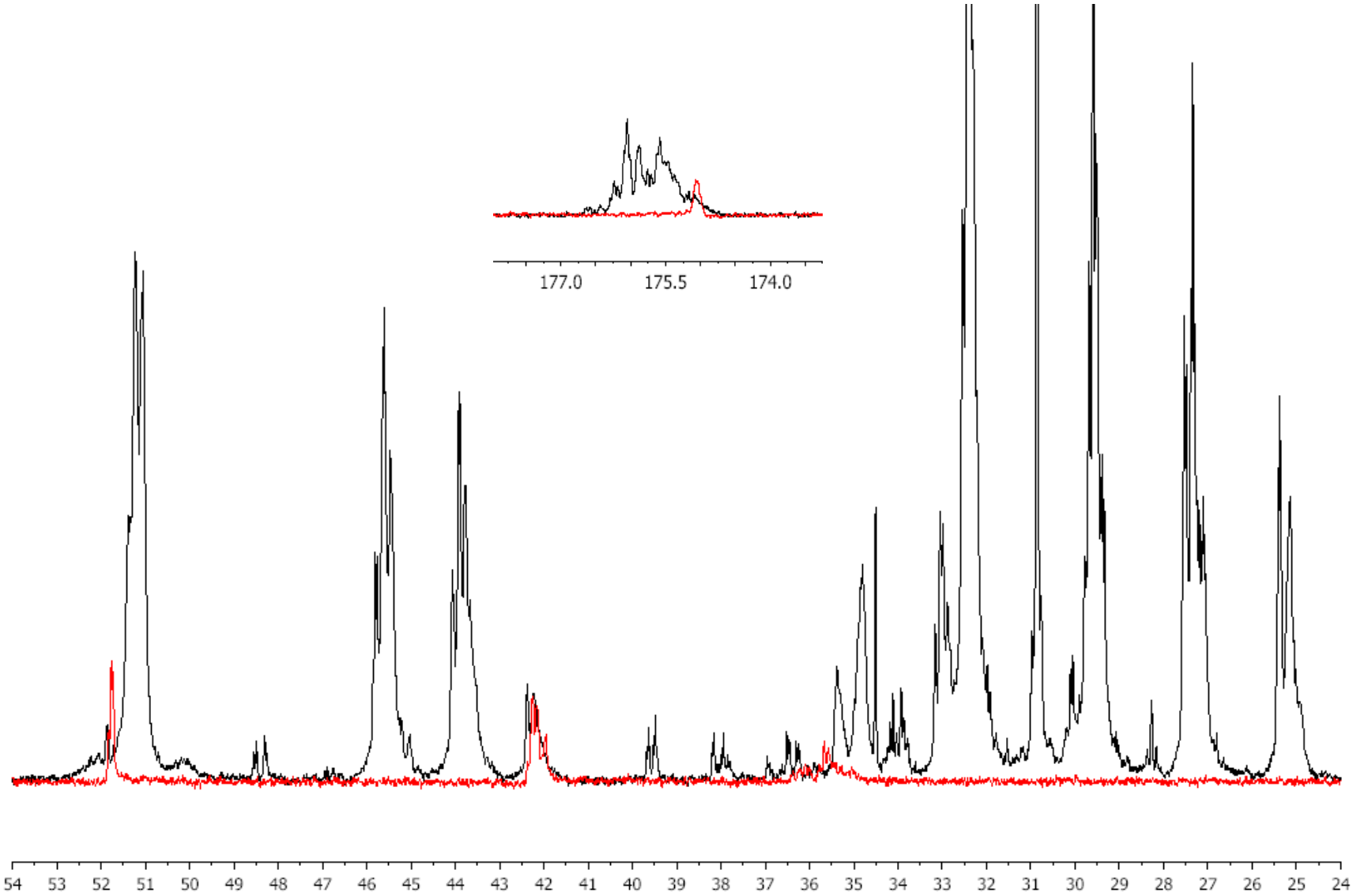

Figure S18. GPC trace of poly(methyl acrylate) obtained by free radical polymerization. Reaction conditions: 50 mg AIBN, 2 mL MA in 4 mL toluene stirred at 70°C for 8h.

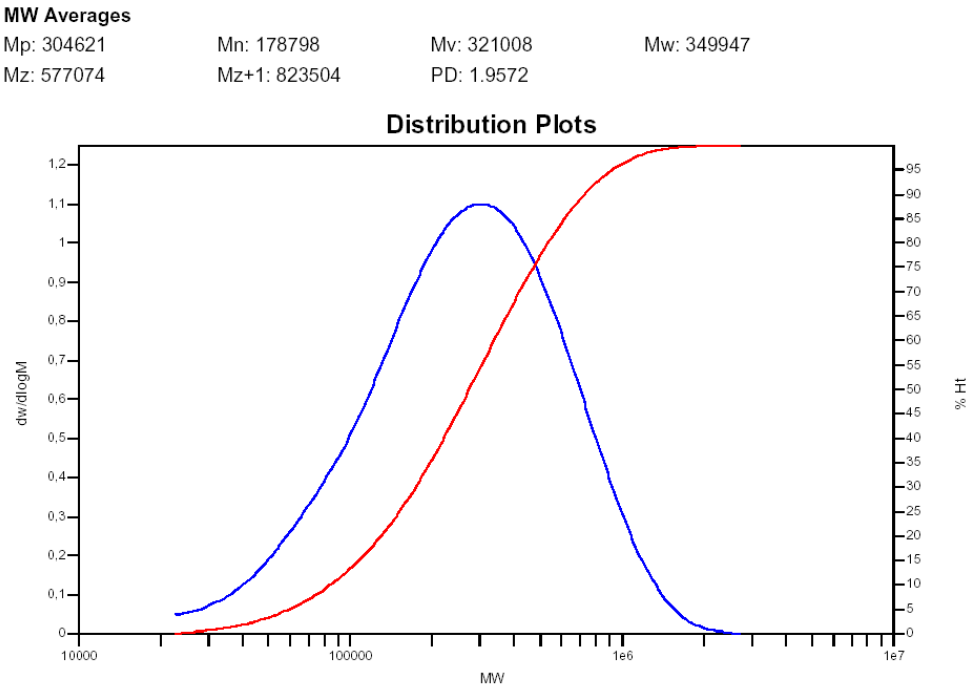

Figure S19. GPC trace of ethylene-methyl acrylate copolymer (entry 2-3). Reaction condition: 20 µmol Pd, 1.2 mol L^{-1} MA, 5 bar ethylene, 95°C for 30 min.

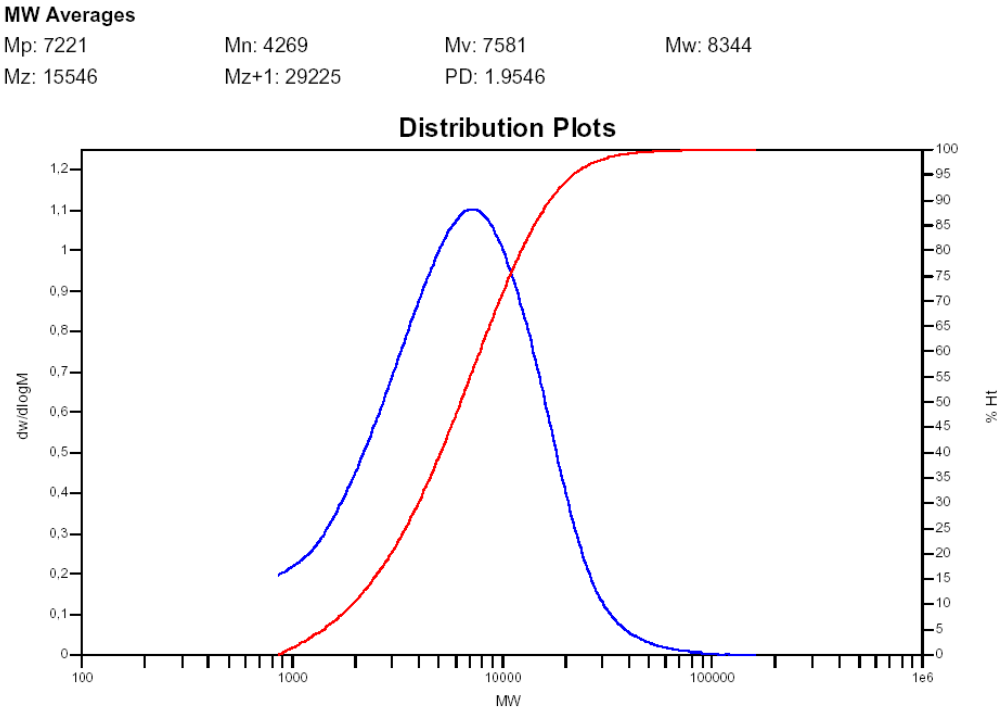

VIII. X-ray diffraction analyses.

A. X-ray crystal structure determination of complex 1a-(κ-O)-(DMSO) • dioxane.

While the sulfonato-group potentially may coordinate in a (κ^2-*O,O*)-fashion, such a coordination mode was not established based on the long Ni1-O2 distance [3.2494(28) Å]. The Ni(II) center is square-planar coordinated, with a 0.0376(17) Å deviation of the metal center from the root mean square plane defined by O1-O6-C1-P1. Note that this is the first X-ray diffraction analysis of a square planar coordinated nickel-sulfoxide complex deposited in the Cambridge Crystallographic Data Centre, and that the Ni1-O6 distance [1.9500(29) Å] is substantially shorter than in hexa- and penta-coordinated (*κ–O*)-sulfoxide nickel complexes [44 octahedral structures, (*κ–O*)-(sulfoxide)Ni(II): 2.042 to 2.253 Å, 1 square-pyramidal structure, (*κ–O*)-(dmso)Ni(II): 2.006 Å (dmso apical)].

Crystallographic data of complex **1a-(*κ–O*)-(dmso) • dioxane**: $C_{27}H_{35}O_8PS_2Ni$, M_r = 641.35 g mol^{-1}, triclinic, space group *P*-1 (no. 2), a = 10.9981(8), b = 12.0103(9), c = 12.0742(10) Å, α = 83.154(6), β = 67.820(6), γ = 88.107(6)°, V = 1466.2(2) Å^3, Z = 2 ρ_{calc} = 1.453 g cm^{-3}, μ ($Mo_{K\alpha}$) = 0.905 mm^{-1}, T = 100 K, yellow-orange rhombohedrus, STOE IPDS 2T, reflections measured: 22479, unique reflections: 6228, *hkl*-range: -13/13, -15/15, -15/15, $2\theta_{max}$ = 53.64°, F^2 refinement, hydrogen atoms are treated in a riding model, dmso-methyl groups are isotropically refined over two split positions with 0.48/0.52 occupancy, parameters: 358, extinction coefficient: 0.0153(15), R_1 =0.0548 for 4307 data ($F_o > 4\sigma(F_o)$), 0.0880 (all data), wR^2 = 0.1264 for 4307 data ($F_o > 4\sigma(F_o)$), 0.1427 (all data), R_{int} = 0.0859, GOF = 1.037, CCDC 697401. Additional data can be obtained free of charge from the Cambridge Crystallographic Data Centre via www.ccdc.cam.ac.uk/data_request/cif.

The data collection was performed at 100 K on a STOE IPDS-II diffractometer equipped with a graphite-monochromated radiation source (λ = 0.71073 Å) and an image plate detection system. A crystal mounted on a fine glass fiber with silicon grease was employed. The selection, integration and averaging procedure of the measured reflex intensities, the determination of the unit cell dimensions by a least-squares fit of the 2Θ values, data reduction, LP-correction and space group determination were performed using the X-Area software package delivered with the diffractometer. A semiempirical absorption correction was performed. The structure was solved by direct methods (SHELXS-97), completed with difference Fourier syntheses, and refined with full-matrix least-squares using SHELXL-97 minimizing $w(Fo^2 - Fc^2)^2$. Weighted R factor (wR) and the goodness of fit GooF are based on F^2; All non-hydrogen atoms except disordered carbon atoms C22 and C23 were refined with anisotropic displacement parameters. Disordered methyl groups C22 and C23 were refined over two split positions whose occupancies minimized to a 0.48:0.52 ratio. All hydrogen atoms were treated in a riding model.

Figure S20. Molecular structure of complex **1a-(κ-*O*)-(DMSO) • dioxane** at the 50% probability level. Hydrogen atoms and cocrystallized dioxane are omitted for clarity.

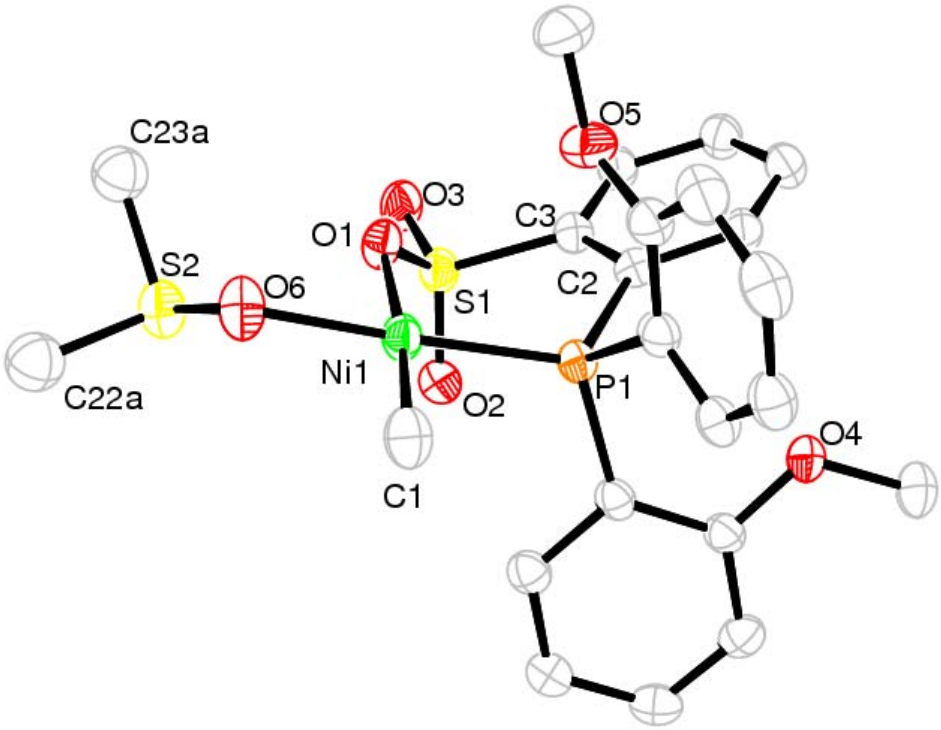

Table S5. Selected (bond) distances [Å] and angles [°] of complex **1a-(*κ-O*)-DMSO**

Ni1-C1	1.9150(43)	C1-Ni1-O6	87.57(16)	C2-C3-S1-O1	51.6(4)
Ni1-O1	1.9765(27)	C1-Ni1-O1	174.84(16)	C3-S1-O1-Ni1	73.6(2)
Ni1-O6	1.9500(29)	C1-Ni1-P1	87.70(13)	S1-O1-Ni1-C1	118.8(19)
Ni1-P1	2.1195(11)	C2-P1-Ni1	112.94(12)	S1-O1-Ni1-P1	40.6(2)
S1-O1	1.4877(29)	P1-C2-C3	121.8(3)	O1-Ni1-P1-C2	115.6(8)
S1-O2	1.4462(30)	C2-C3-S1	121.8(3)	S2-O6-Ni1-P1	170.1(6)
S1-O3	1.4423(27)	C3-S1-O1	104.58(18)	S2-O6-Ni1-C1	136.7(3)
S2-O6	1.5133(30)	S1-O1-Ni1	120.62(16)	S2-O6-Ni1-O1	41.0(2)
P1-C2	1.7780(19)	O1-Ni1-P1	97.14(8)		
C2-C3	1.403(5)	S2-O6-Ni1	117.76(17)		
C3-S1	1.780(4)				
Ni1-O2	3.2494(28)				

deviation of atoms from the root mean square plane defined by O1-O6-C1-P1:

Ni1	-0.0376(17) Å
O1	-0.0679(17)
O6	0.0779(19)
C1	-0.0763(18)
P1	0.0664(16)

dihederal angle defined by the root mean square planes O1-O6-C1-P1 and S1-C3-C2-P1:

31.31(0.12)°

Table S6. Crystallographic Data of Complex **1a-(*κ*–*O*)-(DMSO) • dioxane**

CCDC deposit no	**697401**
Crystal description	dichroic orange-yellow rhombus
Formula	$C_{27}H_{35}NiO_8PS_2$, ($C_{23}H_{27}NiO_6PS_2$ • $C_4H_8O_2$)
Crystal Size [mm^3]	0.15 × 0.1 × 0.05
Crystal System	triclinic
Space group	*P*-1 (2)
a [Å]	10.9981(8)
b [Å]	12.0103(9)
c [Å]	12.0742(10)
α [°]	83.154(6)
β [°]	67.820(6)
γ [°]	88.107(6)
V [$Å^3$]	1466.2(2)
Z	2
M_r [$g \cdot mol^{-1}$]	641.35
ρ_{calc} [$g \cdot cm^{-3}$]	1.453
μ (Mo-Kα) [mm^{-1}]	0.905
F(000) [e]	672
T [K]	100(2)
Wavelenght [Å]	0.71073 (Mo-Kα)
Diffractometer	STOE IPDS 2T
Scan	ω-scan
$\theta_{min-max}$ [°]	1.71-26.82
(sinθ/λ)max [$Å^{-1}$]	63.48
Data total / unique	22479/6228
R_{int}	0.0859
R_{sigma}	0.0731
Data obs ($F^2 \geq 4\sigma(F^2)$)	4307
hkl-range	-13/13, -15/15, -15/15
Absorption correction	numerical Integration[a]
Extinction coefficient[b]	0.0153(15)
Structure Solution	SHELXS-97[c]
Structure Refinement	SHELXL-97[d]
H atoms	constrained
Number Parameters	358
R(F) obs. / all	0.0548/0.0880
wR(F^2) all	0.1264/0.1427
w (*a*, *b*)[e]	0.746, 0
GoF (F^2)	1.037
dU_{max}	0.000
$\Delta\rho_{fin}$ (min./max.) [$e \cdot Å^{-3}$]	0.56/-0.73
remarks	disordered methyl groups C22 and C23 were refined isotropically in split positions (0.48/0.52)

[a] X-RED version 1.31, Stoe Data Reduction Program, Darmstadt, Germany, 2005.

[b] extinction expression: $Fc^* = kF_c[1+0.001*F_c^2\lambda^3/\sin(2\theta)]^{-1/4}$

[c] G. M. Sheldrick, SHELXS-97, Program for Crystal Structure Analysis, Univ. Göttingen, Germany, 1997.

[d] G. M. Sheldrick, SHELXL-97, Program for Crystal Structure Refinement, Univ. Göttingen, Germany, 1997.

[e] weighting scheme: $w = 1/[\sigma^2(Fo^2) + (a \cdot P)^2 + b \cdot P)$, $P = [\max(Fo^2,0) + 2\,Fc^2]/3$.

B. X-ray crystal structure determination of complex 2b-(κ-S)-(DMSO) • ½ Pentane.

While so far (*κ–O*)-coordination is the exclusive coordination mode in crystallographically analyzed Ni-sulfoxide complexes, both (*κ¬S*)- and (*κ–O*)-coordination of sulfoxides in square planar palladium complexes have been reported [the Cambrigde Crystallographic Data Centre contains 34 × (*κ¬S*)-(sulfoxide)-palladium and 12 × (*κ–O*)-(sulfoxide) palladium complexes].[10]

Crystallographic data of complex **2b-(*κ-S*)-DMSO • ½ pentane**: $C_{39.5}H_{45}O_8PS_2Pd$, M_r = 849.24 g mol^{-1}, triclinic, space group *P*-1 (no. 2), a = 10.2115(7), b = 11.9691(7), c = 15.3437(9) Å, α = 96.2445(5), β = 95.976(5), γ = 91.175(5)°, V = 1853.12(2) Å^3, Z = 2 ρ_{calc} = 1.522 g cm^{-3}, μ ($Mo_{K\alpha}$) = 0.710 mm^{-1}, T = 100 K, colourless rhombus, STOE IPDS 2T, reflections measured: 25251, *hkl*-range: -13/13, -15/15, -20/17, $2\theta_{max}$ = 56.84°, F^2 refinement, hydrogen atoms are treated in a riding model, disordered pentane was removed from the structure model by the PLATON SQUEEZE routine before the last least square refinement cycles resulting in 9084 unique reflections, parameters: 451, R_1 =0.0456 for 7162 data ($F_o > 4\sigma(F_o)$), 0.0660 (all data), wR^2 = 0.0851 for 7162 data ($F_o > 4\sigma(F_o)$), 0.0902 (all data), R_{int} = 0.0516, GOF = 1.050, CCDC 073364. Additional data can be obtained free of charge from the Cambridge Crystallographic Data Centre via www.ccdc.cam.ac.uk/data_request/cif.

The data collection was performed at 100 K on a STOE IPDS-II diffractometer equipped with a graphite-monochromated radiation source (λ = 0.71073 Å) and an image plate detection system. A crystal mounted on a fine glass fiber with silicon grease was employed. The selection, integration and averaging procedure of the measured reflex intensities, the determination of the unit cell dimensions by a least-squares fit of the 2Θ values, data reduction, LP-correction and space group determination were performed using the X-Area software package delivered with the diffractometer. A semiempirical absorption correction was performed. The structure was solved by direct methods (SHELXS-97), completed with difference Fourier syntheses, and refined with full-matrix least-squares using SHELXL-97 minimizing w($Fo^2 - Fc^2$)^2. Refinement proceeded to convergence on the ordered part of the structure. At this point residual electron density was detected at the position 0.5, 0.5, 1, which based on NMR analysis of X-Ray quality crystals was identified as 1 molecule of pentane per unit cell (Z =2). However, even considering two site disorder, pentane could not be modeled

satisfactory given by unreasonable bonding distances and angles. Further improvement was achieved using the SQUEEZE routine implemented in PLATON[11] by which 60 e^- were removed from a 168 $Å^3$ solvent accessible void. Results of the SQUEEZE routine are appended at the end of the cif-file. Final R factors, final weighted R factors (wR, based on F^2) and the final goodness of fit GooF (based on F^2) are based on the *hkl*-data obtained from the SQUEEZE routine. All non-hydrogen atoms were refined with anisotropic displacement parameters. All hydrogen atoms were treated in a riding model.

Figure S21. Molecular structure of complex **2b-(κ-*S*)-(DMSO)•½ Pentane** at the 50% probability level. Hydrogen atoms and cocrystallized pentane are omitted for clarity.

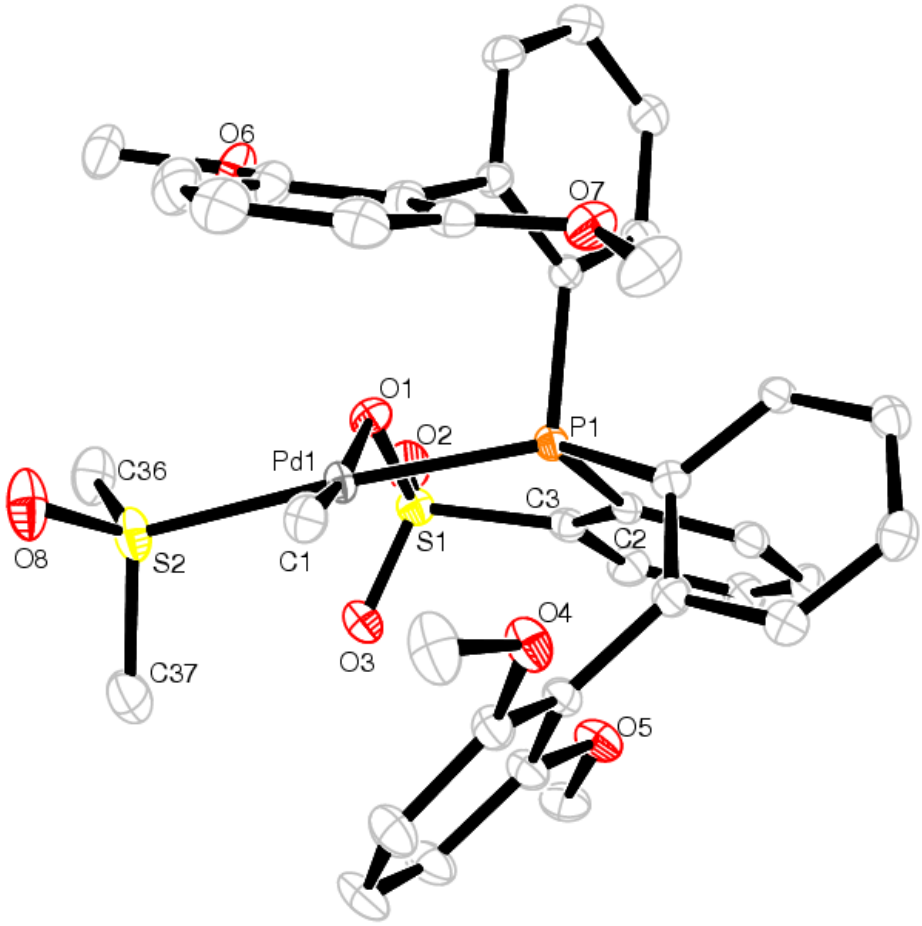

Table S7. Selected (bond) distances [Å] and angles [°]of complex **2b-(*κ*-*S*)-DMSO**

Pd1-C1	2.014(3)	C1-Pd1-S2	86.76(10)	C2-C3-S1-O1	27.9(3)
Pd1-O1	2.178(2)	C1-Pd1-O1	171.07(11)	C3-S1-O1-Pd1	75.97(16)
Pd1-S2	2.3232(9)	C1-Pd1-P1	98.01(10)	S1-O1-Pd1-C1	169.0(7)
Pd1-P1	2.2805(9)	C2-P1-Pd1	111.15(10)	S1-O1-Pd1-P1	82.81(13)
S1-O1	1.475(2)	P1-C2-C3	124.2(2)	O1-Pd1-P1-C2	47.20(12)
S1-O2	1.444(2)	C2-C3-S1	125.2(2)	O8-S2-Pd1-P1	173.4(3)
S1-O3	1.454(2)	C3-S1-O1	106.08(14)	O8-S2-Pd1-C1	34.73(17)
S2-O8	1.478(2)	S1-O1-Pd1	115.23(12)	O8-S2-Pd1-O1	136.43(16)
P1-C2	1.864(3)	O1-Pd1-P1	81.30(6)		
C2-C3	1.409(4)	O8-S2-Pd1	120.93(11)		
C3-S1	1.781(3)				
Pd1-O3	3.197(2)				

deviation of atoms from the root mean square plane defined by O1-S2-C1-P1:

Pd1	-0.0348(11) Å
O1	0.1274(10)
S2	-0.1241(10)
C1	0.1264(10)
P1	-0.1297(10)

dihederal angle defined by the root mean square planes O1-S2-C1-P1 and S1-C3-C2-P1

39.31(7)°

Table S8. Crystallographic Data of Complex **2b-(*κ*–*S*)-(DMSO) • ½ Pentane**

CCDC deposit no	**073364**
Crystal description	colourless rhombus
Formula	$C_{39.5}H_{45}O_8PPdS_2$ ($C_{37}H_{39}O_8PPdS_2$, ½ C_5H_{12})
Crystal Size [mm^3]	0.5 × 0.317 × 0.15
Crystal System	triclinic
Space group	*P*-1 (2)
a [Å]	10.2115(7)
b [Å]	11.9691(7)
c [Å]	15.3437(9)
α [°]	96.244(5)
β [°]	95.976(5)
γ [°]	91.175(5)
V [$Å^3$]	1853.1(2)
Z	2
M_r [$g \cdot mol^{-1}$]	849.24
ρ_{calc} [$g \cdot cm^{-3}$]	1.522
μ (Mo-Kα) [mm^{-1}]	0.710
F(000) [e]	878
T [K]	100
Wavelenght [Å]	0.71073 (Mo-Kα)
Diffractometer	STOE IPDS 2T
Scan	ω-scan
$\theta_{min\text{-}max}$ [°]	2.01-28.42
(sinθ/λ)max [$Å^{-1}$]	0.64
Data total / unique	45185/ 9084
R_{int}	0.0516
R_{sigma}	0.0564
Data obs ($F^2 \geq 4\sigma(F^2)$)	7162
hkl-range	-13/13, -15/15, -20/17
Absorption correction	numerical Integration[a]
Structure Solution	SHELXS-97[b]
Structure Refinement	SHELXL-97[c]
H atoms	constrained
Number Parameters	451
R(F) obs. / all	0.0456/ 0.0660
wR(F^2) all	0.0902
w (*a*, *b*)[d]	0.0260, 3.26
GoF (F^2)	1.050
dU_{max}	0.000
$\Delta\rho_{fin}$ (min./max.) [$e \cdot Å^{-3}$]	1.374/-0.902
remarks	Disordered pentane at 0.5, 0.5, 1 was removed by the PLATON SQUEEZE[e] routine

[a] X-RED version 1.31, Stoe Data Reduction Program, Darmstadt, Germany, 2005.

[b] G. M. Sheldrick, SHELXS-97, Program for Crystal Structure Analysis, Univ. Göttingen, Germany, 1997.

[c] G. M. Sheldrick, SHELXL-97, Program for Crystal Structure Refinement, Univ. Göttingen, Germany, 1997.

[d] weighting scheme: $w = 1/[\sigma^2(Fo^2) + (a \cdot P)^2 + b \cdot P)$, $P = [\max(Fo^2,0) + 2\,Fc^2]/3$.

[e] A. L. Spek, *J. Appl. Cryst.* **2003**, *36*, 7-13

References

(1) de Graff, W.; Boersma, J.; Smeets; Wilberth, J. J.; Spek, A. L.; van Koten, G. *Organometallics* **1989**, *8*, 2907-2917.

(2) Drent, E.; van Dijk, R.; van Ginkel, R.; van Oort, B.; Pugh, R. I. *Chem. Commun.* **2002**, 964-965.

(3) Skupov, K. M.; Marella, P. R.; Simard, M.; Yap, G. P. A.; Allen, N.; Conner, D.; Goodall, B. L.; Claverie, J. P. *Macromol. Rapid Commun.* **2007**, *28*, 2033-2038.

(4) Guironnet, D.; Rünzi, T.; Göttker-Schnetmann, I.; Mecking S. *Chem. Commun.* **2008**, 4965-4967.

(5) Kochi, T.; Noda, S.; Yoshimura, K.; Nozaki, K. *J. Am. Chem. Soc*. **2007**, *129*, 8948-8949

(6) Newsham, D. K.; Borkar, S.; Sen, A.; Conner, D. M.; Goodall, B. L. *Organometallics* **2007**, *26*, 3636-3638.

(7) For examples of Pd(II) chelate complexes cf. (a) Johnson, L. K.; Mecking, S.; Brookhart, M. *J. Am. Chem. Soc.* **1996**, *118*, 267–268; (b) Mecking, S.; Johnson, L. K.; Wang, L.; Brookhart, M. *J. Am. Chem. Soc.* **1998**, *120*, 888–899.

(8) Drent, E.; van Dijk, R.; van Ginkel, R.; van Oort, B.; Pugh, R. I. *Chem. Comm.* **2002**, 774-775.

(9) Liu, S.; Gu, B.; Rowlands, H. A.; Sen, A. *Macromolecules* **2004**, *37*, 7924-7929.

(10) For recent examples, see: (a) (*κ–O*): Molčanov, K.; Ćurić, M.; Babić, D.; Kojić-Prodić, B. *J. Organomet. Chem.* **2007**, *692*, 3874-3881. (b) (*κ–S*): Das, S.; Pal, S. *J. Organomet. Chem.* **2004**, *689*, 352-360.

(11) Spek, A. L. *J. Appl. Cryst.* **2003**, *36*, 7-13.